© 2016. Published by The Company of Biologists Ltd | Journal of Cell Science (2016) 129, 898-911 doi:10.1242/jcs.181180

RESEARCH ARTICLE

α-Dystrobrevin-1 recruits Grb2 and α-catulin to organize neurotransmitter receptors at the neuromuscular junction

Jacinthe Gingras[1,*,§], Marta Gawor[2,§], Krzysztof M. Bernadzki[2], R. Mark Grady[3,‡], Peter Hallock[4], David J. Glass[4], Joshua R. Sanes[1,3] and Tomasz J. Proszynski[2,¶]

ABSTRACT

Neuromuscular junctions (NMJs), the synapses made by motor neurons on muscle fibers, form during embryonic development but undergo substantial remodeling postnatally. Several lines of evidence suggest that α-dystrobrevin, a component of the dystrophin-associated glycoprotein complex (DGC), is a crucial regulator of the remodeling process and that tyrosine phosphorylation of one isoform, α-dystrobrevin-1, is required for its function at synapses. We identified a functionally important phosphorylation site on α-dystrobrevin-1, generated phosphorylation-specific antibodies to it and used them to demonstrate dramatic increases in phosphorylation during the remodeling period, as well as in nerve-dependent regulation in adults. We then identified proteins that bind to this site in a phosphorylation-dependent manner and others that bind to α-dystrobrevin-1 in a phosphorylation-independent manner. They include multiple members of the DGC, as well as α-catulin, liprin-α1, Usp9x, PI3K, Arhgef5 and Grb2. Finally, we show that two interactors, α-catulin (phosphorylation independent) and Grb2 (phosphorylation dependent) are localized to NMJs *in vivo*, and that they are required for proper organization of neurotransmitter receptors on myotubes.

KEY WORDS: Dystrobrevin, AChR, Neuromuscular junction, Maturation, Development, Dystrophin-associated glycoprotein complex

INTRODUCTION

Mammalian neuromuscular junctions (NMJs) form in embryos but undergo intensive remodeling postnatally (Darabid et al., 2014; Sanes and Lichtman, 2001; Shi et al., 2012). Many key components responsible for assembling the postsynaptic apparatus and its acetylcholine receptors (AChRs) have been already identified (Choi et al., 2013; Darabid et al., 2014; Hallock et al., 2010; Shi et al., 2012). Less is known about mechanisms that orchestrate postnatal remodeling of NMJs (Shi et al., 2012); however, the dystrophin-associated glycoprotein complex (DGC) has emerged as a key player. The DGC is a multiprotein transmembrane assembly that connects the extracellular matrix (ECM) surrounding muscle fibers to the intracellular cytoskeleton (Ervasti and Campbell, 1993). Initial interest in the DGC centered on findings that several of its components are mutated in muscular dystrophies (Brown, 1997; Sunada and Campbell, 1995), but it was subsequently shown to play a related role at the NMJ, stabilizing AChRs by anchoring them to the ECM and intracellular cytoskeleton (Ervasti and Campbell, 1993; Jacobson et al., 2001).

Within the DGC, a crucial component is α-dystrobrevin, a cytoplasmic phosphoprotein that binds directly to dystrophin, utrophin and the syntrophins (Peters et al., 1997, 1998; Sadoulet-Puccio et al., 1997). Mice that lack α-dystrobrevin exhibit abnormal distribution, decreased levels and reduced stability of AChRs at the NMJ (Grady et al., 2003, 2000). These defects are primarily attributable to loss of α-dystrobrevin-1, one of several isoforms generated from the α-dystrobrevin gene (*DTNA*) by alternative splicing. α-Dystrobrevin-1 is concentrated at the NMJ, whereas α-dystrobrevin-2 is distributed over the entire muscle fiber, and ectopic expression of α-dystrobrevin-1 but not of α-dystrobrevin-2 fully rescues the synaptic defects observed in α-dystrobrevin-deficient muscle (Newey et al., 2001; Peters et al., 1998; Grady et al., 2003, 2000; Pawlikowski and Maimone, 2009). α-Dystrobrevin-1 and α-dystrobrevin-2 are identical over most of their length, but α-dystrobrevin-1 bears a 176-amino-acid C-terminal extension comprising at least three tyrosine residues that are phosphorylated *in vivo* (Fig. 1A) (Balasubramanian et al., 1998; Blake et al., 1996). Evidence for a role of tyrosine phosphorylation in α-dystrobrevin function came from the demonstration that α-dystrobrevin-1 mutants lacking the three phosphorylatable tyrosine residues were deficient in their ability to stabilize AChRs in the postsynaptic membrane (Grady et al., 2003; Pawlikowski and Maimone, 2009). Moreover, phosphorylation of α-dystrobrevin-1 is controlled by the neuregulin–ErbB signaling pathway (ErbB is also known as EGFR), which itself has been implicated in synaptic remodeling (Schmidt et al., 2011).

Thus, a series of studies have focused attention on tyrosine phosphorylation of α-dystrobrevin-1 as a key regulatory step in synaptic maturation at the NMJ. Here, as a next step, we assayed the roles of three known phosphorylation sites (Y705, Y713, Y730), and identified Y713 and Y730 as key residues for the organization of AChRs. We generated phosphorylation (phospho)-specific antibodies to these sites and used them to demonstrate developmental and nerve-dependent regulation of phosphorylation of α-dystrobrevin-1 at the NMJ. We next identified sets of proteins that interact with α-dystrobrevin-1 in phospho-dependent and -independent manners. Lastly, we demonstrated that two of these proteins, Grb2 and α-catulin, are localized to the NMJ and are required for AChR clustering. Taken together, our studies provide new insights into mechanisms that underlie synaptic maturation and stability.

[1]Department of Molecular and Cellular Biology and Center for Brain Science, Harvard University, Cambridge, MA 02138, USA. [2]Laboratory of Synaptogenesis, Dept. of Cell Biology, Nencki Institute of Experimental Biology, Warsaw 02-093, Poland. [3]Department of Anatomy and Neurobiology, Washington University School of Medicine, St Louis, MO 63110, USA. [4]Novartis Biomedical Institute, Cambridge, MA 02139, USA.
*Present address: Department of Neuroscience, Amgen Inc., Cambridge, MA 02142, USA. ‡Present address: Department of Pediatrics Cardiology, Washington University School of Medicine, St. Louis, MO 63110, USA.
§These authors contributed equally to this work

¶Author for correspondence (t.proszynski@nencki.gov.pl)

Received 2 October 2015; Accepted 11 January 2016

Journal of Cell Science (2016) 129, 898-911 doi:10.1242/jcs.181180

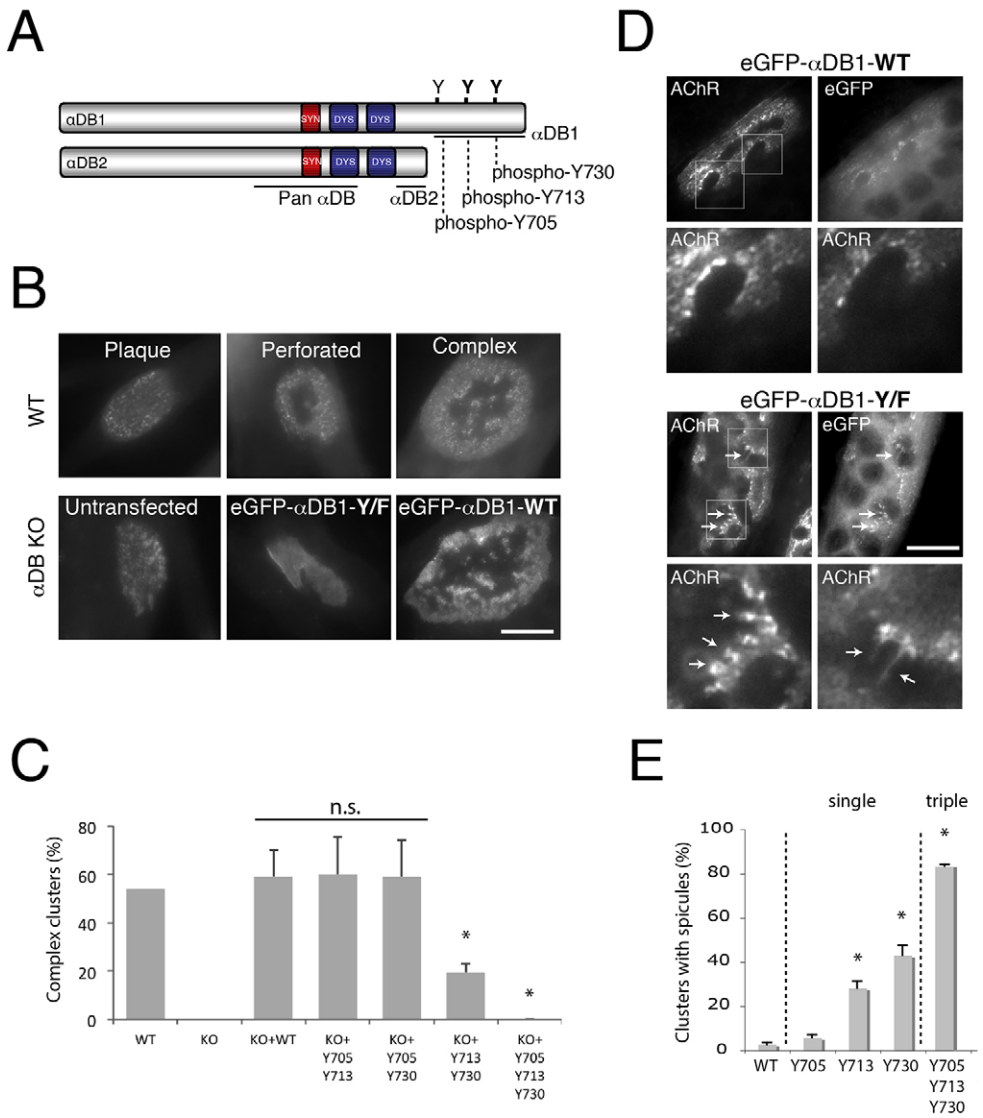

Fig. 1. Identification of α-dystrobrevin-1 phosphorylation sites involved in postsynaptic maturation. (A) Schematic illustration of α-dystrobrevin-1 (αDB1) and α-dystrobrevin-2 (αDB2) isoforms. The α-dystrobrevin-1 C-terminus bears three tyrosine residues (Y) that can be phosphorylated (Y705, Y713, Y730). Both α-dystrobrevin isoforms contain syntrophin- (red) and dystrophin- (blue) binding domains. (B) Primary myotubes assemble plaques of AChRs that become perforated and mature into complex clusters. Myotubes from α-dystrobrevin-KO (αDB KO) cells form plaques that fail to mature (untransfected). Maturation can be rescued by introduction of wild-type (WT) α-dystrobrevin-1 (eGFP–αDB1-WT), but not mutant α-dystrobrevin-1 (eGFP–αDB1-Y/F) in which Y705, Y713 and Y730 have been mutated to phenylalanine (F) and are unphosphorylatable. (C) Residues Y713 and Y730 are required for the formation of complex clusters. Primary myotubes derived from WT or α-dystrobrevin-KO (KO) myoblasts were transfected with either eGFP–αDB1-WT or mutated α-dystrobrevin-1 constructs and analyzed for their ability to form complex clusters of AChRs. Y705, Y713 and Y730 indicate the mutated residues. Residues Y713 and Y730 are the most crucial for the proper organization of AChR clusters, as shown by the ~68% decrease in complex clusters quantified [WT: 54%, *n*=76; αDB-KO: 0%, *n*=77; αDB-KO+eGFP–αDB1-WT (KO+WT): 59%, *n*=29; αDB-KO+eGFP–αDB1-Y705-Y713 (KO+Y705 Y713): 60%, *n*=42; αDB-KO+eGFP–αDB1 Y705-Y730 (KO+Y705 Y730): 59%, *n*=31; αDB-KO+eGFP–αDB1-Y713-Y730 (KO+Y713 Y730): 19%, *n*=63; αDB-KO+eGFP–αDB1-Y/F (KO+Y705 Y713 Y730): 0%, *n*=19]; **P*<0.05 (two-tailed Student *t*-test, mean±s.d.). The percentage of complex clusters was calculated from five independent experiments (each 2–4 wells per construct). n.s., not significant. (D) C2C12 myotubes overexpressing either eGFP–αDB1-WT or the triple mutated (eGFP–αDB1-Y/F) α-dystrobrevin-1 construct were analyzed for aberrations in AChR cluster integrity. Lower images in each set show magnification of the areas boxed in the upper images (AChR channel). Arrows indicate AChR-rich spicules protruding from the edges of the assemblies. (E) Ectopic expression of single mutants in C2C12 myotubes revealed that mutation of residues Y713 and Y730 had the strongest effect on cluster organization. An increasing appearance of spicules was observed in complex clusters bearing Y713, Y730 and Y/F triple mutations (Y705: 5.76%±1.35; Y713: 28.22%±3.26 (*P*=0.004); Y730: 43.05%±4.56 (*P*=0.0003); αDB1-Y/F (Y705, Y713, Y730): 83.66%±0.64 (*P*=0.0001). The percentage of clusters with spicules was calculated from three independent experiments, and at least *n*=20 clusters were analyzed per each construct (**P*<0.05, one-tailed Student *t*-test, mean±s.d.). Scale bars: 10 µm.

RESULTS

α-Dystrobrevin-1 phosphorylation at positions Y713 and Y730 is required for remodeling of the postsynaptic membrane

To begin this study, we assessed the role of the three known sites of α-dystrobrevin-1 tyrosine phosphorylation (Y705, Y713, Y730) in AChR clustering (α-dystrobrevin-1 and α-dystrobrevin-2 sequences according to Uniprot IDs Q9D2N4-1 and Q9D2N4-3, respectively; Fig. 1A). To this end, we cultured myoblasts from wild-type (WT) or α-dystrobrevin-knockout (α-dystrobrevin-KO) mice, generated myotubes and transfected the myotubes with vectors encoding wild-type or mutant α-dystrobrevin-1 in which Y705, Y713 and Y730 had been mutated to phenylalanine. To visualize AChRs, we stained myotubes with fluorescently labeled α-bungarotoxin (BTX). When

Journal of Cell Science (2016) 129, 898-911 doi:10.1242/jcs.181180

wild-type myotubes are cultured on laminin-coated surfaces, their AChRs initially form simple plaque-like clusters that then become perforated and eventually form complex pretzel-like shapes that resemble mature NMJs *in vivo* (Kummer et al., 2004). In contrast, AChRs on α-dystrobrevin-1-deficient myotubes formed unperforated simple clusters that failed to mature into more complex assemblies (Fig. 1B; Fig. S1). Consistent with previous results (Pawlikowski and Maimone, 2009), expression of a GFP–α-dystrobrevin-1 fusion protein (GFP–αDB1-WT) in α-dystrobrevin-1-deficient myotubes restored their ability to form complex AChR aggregates, whereas expression of a fusion protein with the three known sites of tyrosine phosphorylation mutated to phenylalanine (GFP–αDB1-Y/F) was ineffective (Fig. 1B,C). We then tested vectors in which pairs of phosphorylation sites were mutated. If both Y713 and Y730 were mutated, rescue was severely compromised, whereas if either was intact, rescue was complete (Fig. 1C). Thus, tyrosine residues Y713 and Y730 appear to play more substantial roles than Y705 in the rescue of AChR clustering in α-dystrobrevin-KO myotubes *in vitro*.

As a second test, we asked whether overexpression of α-dystrobrevin-1 tyrosine mutants in myotubes derived from C2C12 myoblasts affected the architecture of AChR clusters. Expression of the triple mutant (GFP–αDB1-Y/F) led to disruption of cluster morphology, presumably through a dominant-negative mechanism, in which mutant α-dystrobrevin-1 displaced wild-type α-dystrobrevin-1 from crucial complexes. In these myotubes, AChR-rich spicules frequently protruded from the clusters (Fig. 1D, arrows), a defect similar to that observed in α-dystrobrevin-1 mutant NMJs *in vivo* (Grady et al., 2003, 2000). Introduction of the Y713F and Y730F single mutants resulted in similar defects, whereas introduction of the Y705F mutant or wild-type α-dystrobrevin-1 had no significant effect (Fig. 1E). This result supports the conclusion that residues Y713 and Y730 are important for AChR clustering.

We also used the GFP–αDB1 fusion proteins to test the possibility that tyrosine mutation acts by preventing incorporation of α-dystrobrevin-1 into AChR clusters. However, single, double and triple tyrosine mutants all localized to clusters as well as the wild-type α-dystrobrevin-1 protein did (Fig. 1D).

Generation and characterization of phospho-specific α-dystrobrevin-1 antibodies

To analyze the regulation of α-dystrobrevin-1 tyrosine phosphorylation, we generated antisera to phosphopeptides that contained the two tyrosine sites that had been defined in our mutagenesis study and purified phospho-specific antibodies from the sera [against phospho-Y713 and phospho-Y730]. To assess the specificity of the antibody, we first expressed N-terminally GFP-tagged wild-type or triple-mutant α-dystrobrevin-1 (eGFP–αDB1 or eGFP–αDB1-Y/F) in HEK293 cells. To prevent dephosphorylation of the protein by endogenous phosphatases, we treated the cells with the phosphatase inhibitor pervanadate. To ensure that the protein was phosphorylated, we immunoprecipitated α-dystrobrevin-1 from transfected HEK293 cell lysates and probed the precipitate with a well-characterized antibody against phosphotyrosine residues (Fig. S2A). With this assurance, we stained transfected cells with our purified antibodies against phospho-Y713 and phospho-Y730. Both antibodies labeled cells that had been transfected with eGFP–αDB1 but not those transfected with eGFP–αDB1-Y/F (Fig. 2A; Fig. S2B); staining of cells that had been transfected with eGFP–αDB1 was barely detectable if pervanadate was omitted (not shown). We also probed transfected HEK293 cell lysates by western blotting and found that the antibodies against phospho-Y713 and phospho-Y730 recognized phosphorylated wild-type α-dystrobrevin-1 but not the tyrosine mutant (Fig. 2B, see also Fig. 4C later). Thus, our antibodies against phospho-α-dystrobrevin-1 recognized native and denatured phosphorylated α-dystrobrevin-1.

Phosphorylation of α-dystrobrevin-1 increases during synaptic maturation

We used the antibodies against phospho-Y713 and phospho-Y730 to assess the phosphorylation state of α-dystrobrevin-1 at postsynaptic sites. Antibodies against α-dystrobrevin-1, phospho-Y713 and phospho-Y730 all stained AChR-rich aggregates in cultured myotubes (Fig. 2C). Likewise, the antibody against phospho-Y713 selectively stained AChR-rich branches of adult NMJs (Fig. 2D). This immunolabeling was specific because it was not observed at NMJs from α-dystrobrevin-knockout mice. Similar results were obtained with the antibody against phospho-Y730, but staining was weaker and less consistent (data not shown), so we focused on phospho-Y713 in subsequent studies. Immunoreactivity was specific in that neither antibody stained NMJs in α-dystrobrevin-KO mutants (Fig. 2D; data not shown).

We next assessed the phosphorylation of α-dystrobrevin-1 at Y713 at developing NMJs. Total α-dystrobrevin-1 levels increased gradually during the first seven postnatal weeks (Fig. 2E). In striking contrast, α-dystrobrevin-1 that had been phosphorylated at Y713 was undetectable at NMJs in neonates. Levels of phospho-Y713 α-dystrobrevin-1 then increased dramatically over the first two postnatal weeks, peaking at postnatal day (P)14 and declining modestly to a plateau that was sustained into adulthood (Fig. 2E). Taken together, these data indicate that phosphorylation of a crucial tyrosine residue on α-dystrobrevin-1 increases during the period that the NMJ is remodeled postnatally.

α-Dystrobrevin-1 phosphorylation is regulated by innervation

AChR levels at NMJs decrease, and turnover increases following denervation of adult muscle, mirroring defects observed in α-dystrobrevin-KO mutant mice (Loring and Salpeter, 1980). We therefore considered the possibility that nerves act, in part, by regulating the levels of α-dystrobrevin-1 phosphorylation. To test this idea, we analyzed synaptic sites in the denervated sternomastoid muscle by cutting the accessory nerve that innervates it. The levels of total α-dystrobrevin were little changed after denervation (Fig. 2G), but the levels of α-dystrobrevin-1 phosphorylated at Y713 declined approximately 75% within 3 days and then continued to decline gradually over the next 3 weeks, as evaluated by calculating the average pixel intensity of staining with the antibody against phospho-Y713 (Fig. 2F). Thus, α-dystrobrevin-1 phosphorylation is nerve-innervation dependent.

We asked whether the decline in α-dystrobrevin-1 phosphorylation is reversible. To this end, we crushed the nerve to the sternomastoid rather than cutting it. Denervation is long-lasting following nerve cutting, but reinnervation begins with ~3 days following nerve crush near the muscle's edge (Loring and Salpeter, 1980; Salpeter et al., 1986). After nerve crush, the level of phosphorylated α-dystrobrevin-1 dropped significantly reaching its lowest level at P3. It rose again after nerve reinnervation of the tissue at P5, as evaluated by calculating the average pixel intensity of staining with the antibody against phospho-Y713 (Fig. 2F). These results support the conclusion that α-dystrobrevin-1 phosphorylation is neurally regulated.

Journal of Cell Science (2016) 129, 898-911 doi:10.1242/jcs.181180

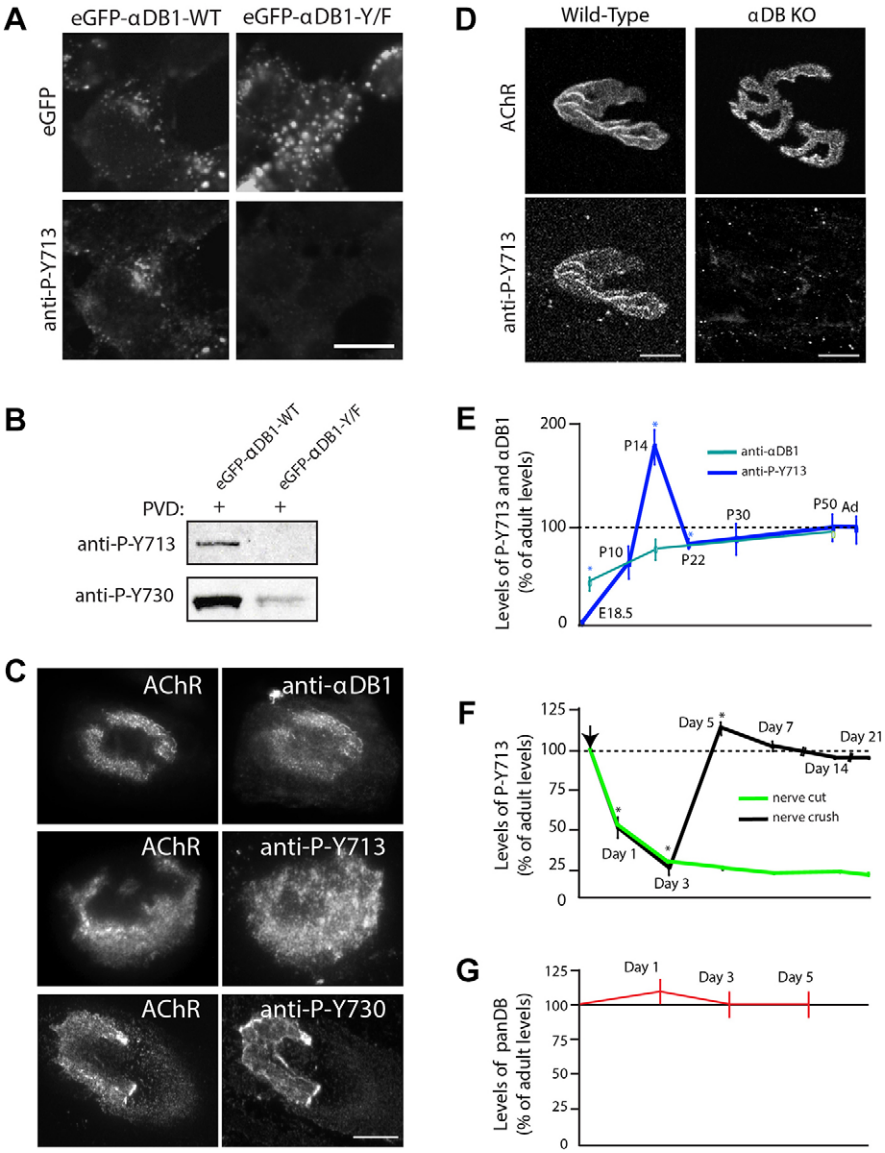

Fig. 2. Dystrobrevin phosphorylation is dynamically regulated during postsynaptic remodeling. (A,B) Evaluation of phospho-specific antibodies. (A) Phospho-Y713 immunofluorescence was detected in HEK293 pervanadate (PVD)-treated cells expressing eGFP–αDB1-WT but not eGFP–αDB1-Y/F. Expression of the corresponding proteins is confirmed by the eGFP signal. Scale bar: 10 µm. (B) Lysates from PVD-treated HEK293 cells that had been transfected with indicated α-dystrobrevin-1 constructs were used to precipitate α-dystrobrevin-1, and the level of phosphorylation was analyzed with the antibodies against the specific phospho-tyrosine residues (anti-P-Y713 and anti-P-Y730) by western blotting (see also Fig. S2). (C) Localization of total α-dystrobrevin-1 and α-dystrobrevin-1 phosphorylated at positions Y713 and Y730 at AChR clusters in C2C12 cells visualized using the indicated antibodies. Scale bar: 15 µm. (D) Localization of phospho-Y713 α-dystrobrevin-1 (anti-P-Y713) at the NMJ. Scale bar: 12 µm. (E) α-dystrobrevin-1 phosphorylation is regulated during developmental remodeling of NMJs. Levels of expression were as follows: anti-P-Y713 [E18.5: 0%±0 (P=0.032); P10: 85.39%±18.34 (P=0.628); P14: 205.57%±19.30 (P=0.032); P22: 103.89%±8.37 (P=0.043); P30: 98.14%±21.66 (P=0.939); P50: 97.98%±9.63 (P=0.854) (two-tailed Mann–Whitney U test, mean±s.e.m.)]; anti-α-dystrobrevin-1 (αDB1) [P0: 61.05%±2.26; P14: 80.5%±8.48; adult (Ad): 100%]. Asterisk indicates statistical significance of P<0.05. Total number of NMJs (n=30) was analyzed from three animals per group. (F) Denervation leads to a decrease in α-dystrobrevin-1 phosphorylation. Immunohistochemical analysis of anti-P-Y713 levels after denervation (nerve cut and crush) of sternomastoid muscle compared to control, extracted from the uninjured contralateral side of the same animal (day 1: P=0.009; day 3: P=0.009; day 5: P=0.0209; day 7: P=0.248; day 14: P=0.337; day 21: P=0.248) (one-tailed Mann–Whitney U test, mean±s.e.m.). Asterisk indicates statistical significance of P<0.05. The total number of NMJs (n=30) was analyzed from three animals per group. Arrow indicates surgical intervention. (G) The total level of all α-dystrobrevin isoforms at the synapses after nerve injury analyzed by immunofluorescence with a pan- dystrobrevin (panDB) antibody. Values from denervated tissues are shown as normalized to the control tissue (un-injured contralateral muscle from the same animal). Mean±s.e.m.

Identification of α-dystrobrevin-1-interacting proteins

To identify proteins that bind to α-dystrobrevin-1, we expressed tandem affinity purification (TAP)-tagged α-dystrobrevin-1 in C2C12 myotubes, purified α-dystrobrevin-1-containing complexes and separated them by using gel electrophoresis. Both the control and α-dystrobrevin-1 samples were divided into eight distinct protein samples, digested with trypsin and subjected to microcapillary reverse-phase HPLC nano-electrospray tandem mass spectrometry (µLC-MS-MS) for protein identification (Fig. 3A).

We identified 25 proteins that had been co-purified with α-dystrobrevin-1 using the criterion of eight or more peptides

Journal of Cell Science (2016) 129, 898-911 doi:10.1242/jcs.181180

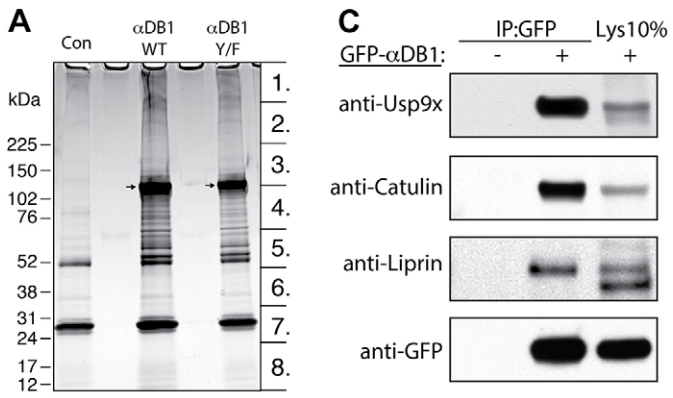

B

Protein name	MS/MS spectra -WT	MS/MS spectra -Y/F	Coverage (%)	Unique peptides	Fraction concentr
αDB1	1835	1604	92.4	180	3-4
Syntr.-α1	302	292	73.7	53	5-6
Syntr-β1	332	330	76.9	63	5-6
Syntr.-β2	102	83	56.9	28	5-6
Utrophin	189	252	40.2	127	1
βDB1	17	20	3.9	3	3-6
Catulin	**92**	**97**	**46**	**29**	4
Usp9x	**79**	**113**	**19**	**48**	1-2
Liprin-α1	**8**	**9**	**7.4**	**7**	3

Fig. 3. Identification of general α-dystrobrevin-1-binding proteins in myotubes. (A) SDS-PAGE gel of proteins that co-purified with TAP–GFP–αDB1 from C2C12 myotubes. Segments numbered 1–8 show regions analyzed individually with mass spectrometry. Con, control sample obtained from uninfected myotubes; αDB1-WT, sample from myotubes infected with TAP–αDB1-WT virus; αDB1-Y/F sample from myotubes infected with TAP–αDB1-Y/F virus. Arrows indicate αDB1 proteins. (B) Subset of interacting proteins identified with mass spectrometry. Proteins that have not previously been shown to interact with αDB1 are in bold. 'MS/MS spectra' for the WT and Y/F constructs represent the total number of peptides identified for each protein; 'coverage' represents the percentage of the protein sequence by identified peptides; 'unique peptides' represent the number of unique peptides for a given protein. Fraction concentr , fractions of the gel lane (indicated in Fig. 1A) in which protein was detected. (C) Tests of interaction by co-precipitating proteins. Epitope-tagged GFP–αDB1 was transfected into HEK293 cells. Lysates from transfected or untransfected cells (control) were used for immunoprecipitation (IP) with an anti-GFP antibody, and precipitates were analyzed by western blotting (WB) for the indicated proteins. 10% of the lysate (Lys 10%) used for the precipitation experiments was loaded into the gel as a control (right lanes). Syntr., syntrophin.

detected in the α-dystrobrevin-1 complexes than in the corresponding control fraction. Fifteen of the interacting proteins are known to participate in protein translation, cellular stress response and protein degradation. Although these proteins might bind to α-dystrobrevin-1, we reasoned that their association was likely to be a nonspecific consequence of α-dystrobrevin-1 overexpression, which would lead to an artificially large translational pool and stimulate cellular stress, sequestration and degradation. The one protein from this group that we considered further was the deubiquitinating enzyme Usp9x (Théard et al., 2010), which was highly enriched in α-dystrobrevin-1 complexes (79 peptides recovered) and virtually missing in the control purification. The remaining eight proteins comprised six components of the DGC [three syntrophin isoforms, two dystrobrevin isoforms and utrophin (Sunada and Campbell, 1995)]; α-catulin, which we and others have previously shown to bind to α-dystrobrevin (Lyssand et al., 2010; Oh et al., 2012); and liprin-α1, a scaffold protein previously shown to interact with α-catulin (Lyssand et al., 2010; Spangler and Hoogenraad, 2007; Spangler et al., 2011) (Fig. 3B).

To validate these interactions, we co-transfected HEK293 cells with plasmids encoding eGFP–αDB1 and the candidate interacting protein, precipitated eGFP–αDB1 from lysates and asked whether the interacting protein was present in the precipitate. This method confirmed interaction of α-dystrobrevin-1 with α-catulin, liprin-α1 and Usp9x (Fig. 3C).

Purification of phospho-specific α-dystrobrevin-1-interacting proteins

To identify proteins that interacted with α-dystrobrevin-1 in a phospho-specific manner, we repeated the TAP affinity purification using the αDB1-Y/F construct (three tyrosine residues replaced by phenylalanine) and compared the interacting proteins to those proteins interacting with full-length α-dystrobrevin-1. We found no significant differences between the two complexes (data not shown), probably because only a small fraction of the full-length isoform was phosphorylated under the conditions we used. We therefore adopted a peptide-based approach (Hallock et al., 2010; Schulze and Mann, 2004). We generated two peptides corresponding to amino acids 706–720 of α-dystrobrevin-1; residue Y713 was phosphorylated in one peptide and was unphosphorylated in the other. Peptides were immobilized, incubated with lysates from C2C12 myotubes, washed and fractionated by using gel electrophoresis (Fig. 4A). Gel slices were then subjected to mass spectrometry analysis as above. We identified 12 proteins that interacted with the phospho-Y713 peptide but not the unphosphorylated peptide (Fig. 4B): Grb2, an SH2- and SH3-domain-containing adaptor protein that interacts with cell surface receptors and signaling machinery (Giubellino et al., 2008); five subunits of phosphatidylinositol 3-kinases (Acebes and Morales, 2012); Arhgef2 and Arhgef5, guanine nucleotide exchange factor (GEFs) for Rho (Kuroiwa et al., 2011; Siesser et al., 2012); SH3-domain-binding protein 2 (SH3BP2), which binds to SH3 domains of proteins of signal transduction pathways (Reichenberger et al., 2012); SH2B, an adaptor protein for several receptor tyrosine kinases (Song et al., 2010); and Fer and Hck, tyrosine-protein kinases that regulate the actin cytoskeleton, cellular adhesion, migration and signaling (Cougoule et al., 2010; Greer, 2002). Eight of these proteins contain an SH2 domain that is responsible for binding to phospho-tyrosine residues in a sequence-specific manner (Schulze and Mann, 2004).

We analyzed interactions of a subset of these proteins. First, we co-expressed Grb2, Fyn or α-catulin with eGFP-tagged wild-type or tyrosine mutant α-dystrobrevin-1, and found that Grb2 and Fyn co-immunoprecipitated only with the wild-type protein (Fig. 4D). α-Catulin, which binds in a phospho-independent fashion (see above) was precipitated by both wild-type and mutant α-dystrobrevin-1 (Fig. 4D). Second, we co-transfected HEK293 cells with dominant-active Src and pre-treated cells with pervanadate to maintain a high level of α-dystrobrevin-1 tyrosine phosphorylation. GFP–αDB1 was precipitated from HEK293 lysate and increased α-dystrobrevin-1 phosphorylation was confirmed using the antibody recognizing phospho-Y713 and an antibody recognizing pan-phospho-tyrosine residues (Fig. 4C). We observed that an increase in α-dystrobrevin-1 phosphorylation correlated with an augmented degree of Grb2 binding to α-dystrobrevin-1 (Fig. 4D). To investigate whether the interacting proteins that we had identified bound directly to phosphorylated α-dystrobrevin-1, we purified GFP-tagged wild-type and mutant α-dystrobrevin-1 from HEK293

Journal of Cell Science (2016) 129, 898-911 doi:10.1242/jcs.181180

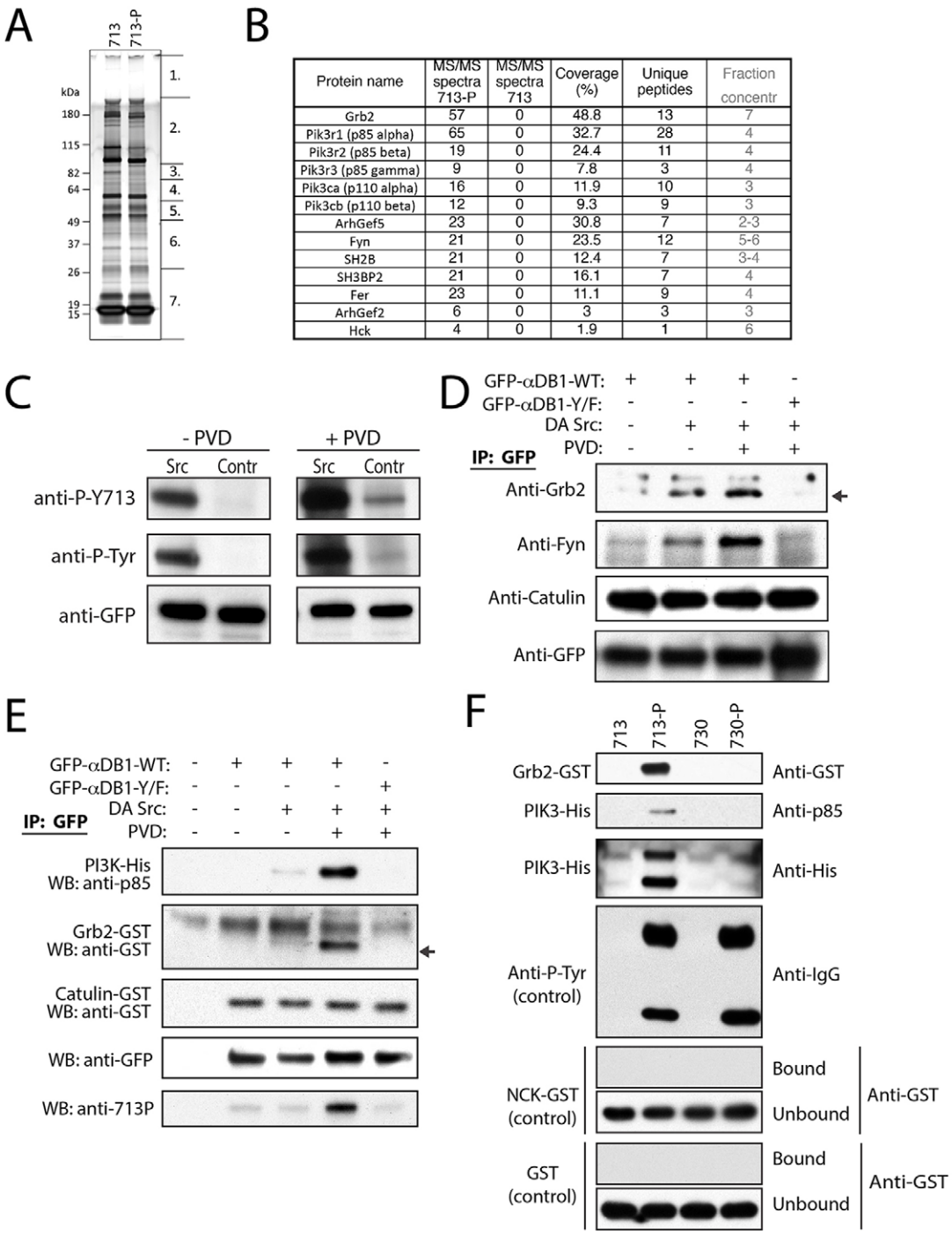

Protein name	MS/MS spectra 713-P	MS/MS spectra 713	Coverage (%)	Unique peptides	Fraction concentr
Grb2	57	0	48.8	13	7
Pik3r1 (p85 alpha)	65	0	32.7	28	4
Pik3r2 (p85 beta)	19	0	24.4	11	4
Pik3r3 (p85 gamma)	9	0	7.8	3	4
Pik3ca (p110 alpha)	16	0	11.9	10	3
Pik3cb (p110 beta)	12	0	9.3	9	3
ArhGef5	23	0	30.8	7	2-3
Fyn	21	0	23.5	12	5-6
SH2B	21	0	12.4	7	3-4
SH3BP2	21	0	16.1	7	4
Fer	23	0	11.1	9	4
ArhGef2	6	0	3	3	3
Hck	4	0	1.9	1	6

Fig. 4. Identification of phospho-specific α-dystrobrevin-1-interacting proteins in myotubes. (A) SDS-PAGE gel of proteins co-purified with peptides 713-P (phospho-Y713 peptide) and 713 (unphosphorylated Y713 peptide, control). Segments numbered 1–7 show regions analyzed individually with mass spectrometry. (B) Proteins specifically interacting with the phospho-Y713 peptide (MS-MS spectra for 713=0) identified by mass spectrometry. MS/MS spectra, total number of peptides identified for each protein. (C) Co-transfection of GFP–αDB1 with a dominant-active (DA) mutant of Src and treatment with pervanadate (PVD) increased the level of α-dystrobrevin-1 phosphorylation (P-Y713, phospho-Y713; P-Tyr, pan phosphorylated tyrosine). Contr, control. (D) Grb2 and Fyn co-precipitate with phosphorylated α-dystrobrevin-1, whereas interaction of α-dystrobrevin-1 with α-catulin was phosphorylation independent. Indicated α-dystrobrevin-1 proteins were precipitated from HEK293 cell lysate, and purification of binding partners was analyzed by western blotting for the indicated proteins. Arrow indicates Grb2-specific band. IP, immunoprecipitation. (E) Tests of phosphorylated α-dystrobrevin-1 interaction with PI3K and Grb2 by protein pull down. The indicated α-dystrobrevin-1 proteins were purified from HEK293 cells in the presence or absence of dominant-active Src mutant and PVD as indicated. Purified α-dystrobrevin-1 was incubated in the presence of purified recombinant PI3K–His, Grb2–GST or α-catulin–GST. Subsequently, α-dystrobrevin-1 was precipitated, and the recovered proteins were analyzed by western blotting for the indicated proteins and phospho-Y713 (713P). Arrow indicates the GST- (Grb2) specific band. (F) Tests for protein affinity for the phosphorylated Y713 and Y730 sites of α-dystrobrevin-1. Synthetic phosphorylated peptides corresponding to the Y713 and Y730 sites (713-P and 730-P), or unphosphorylated peptides (713 and 730, controls) were analyzed for their ability to precipitate Grb2–GST or PI3K–His (complex of the p85 and p110 subunits) purified recombinant proteins; indicated on the left side of the panel. Antibodies against pan-phosphorylated tyrosine residues (anti-P-Tyr), unrelated SH2-domain containing protein GST–NCK or GST were used as controls. After precipitation, the proteins recovered using the biotinylated-peptide–protein complex were analyzed by western blotting for the proteins indicated on the right side of the panel.

Journal of Cell Science (2016) 129, 898-911 doi:10.1242/jcs.181180

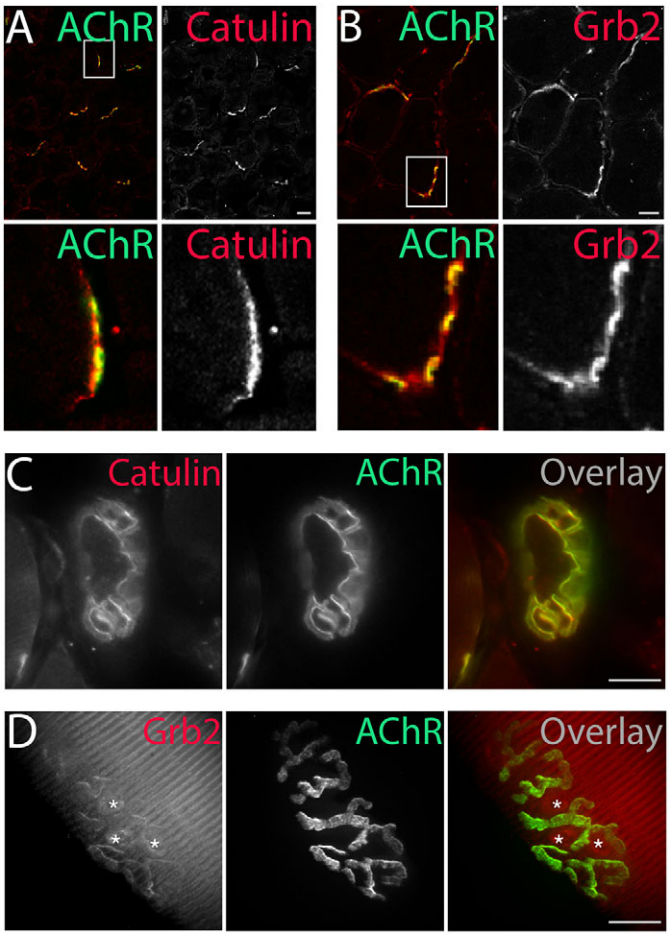

Fig. 5. Localization of α-dystrobrevin-1-interacting proteins to the NMJ. α-Catulin (A) and Grb2 (B) (antibodies, red) concentrate at the postsynaptic machinery of NMJs (AChR, green), as visualized by immunohistochemical analysis of 6-µm-thick slices of tibialis anterior muscle. Immunostaining of α-catulin in the triangularis sternum muscle (C) and Grb2–GFP fluorescence in the tibialis anterior muscle (D) (both shown in red) mirrored the localization of AChRs (green). Asterisks in D indicate fluorescence at synaptic nuclei (see also Fig. 6B). Scale bars: 20 µm.

cells that expressed dominant-active Src (to increase α-dystrobrevin phosphorylation). We used dissociating conditions that disrupt most protein interactions. The purified proteins were then incubated with purified recombinant epitope-tagged Grb2 or PI3K. Both PI3K and Grb2 bound directly to phosphorylated full-length α-dystrobrevin-1 but not to unphosphorylated α-dystrobrevin-1 or the α-dystrobrevin-1 mutant (Fig. 4E). Next, to determine whether binding was specific to phospho-Y713 α-dystrobrevin-1, we used non-phosphorylated and phosphorylated peptides corresponding to both the Y713 and Y730 phosphorylation sites, and asked whether purified recombinant Grb2 and PI3K bound specifically to Y713. Grb2 and PI3K bound to the phospho-Y713 peptide but not to the pY730 peptide (Fig. 4F). In contrast, both phosphorylated peptides were precipitated by the antibody against pan-phospho-tyrosine residues, whereas neither of the phospho-peptides interacted detectably with GST alone or with NCK, an SH2-domain-containing protein that was not identified as a α-dystrobrevin-1 interactor (Fig. 4F). Taken together, these results demonstrate that phosphorylation of α-dystrobrevin-1 acts to recruit a set of signaling molecules that could underlie its ability to regulate postsynaptic remodeling.

α-Catulin and Grb2 are enriched at neuromuscular synapses

For subsequent studies, we focused on one phospho-independent α-dystrobrevin-1 interacting protein, α-catulin, and one phospho-dependent interactor, Grb2. We found that both α-catulin and Grb2 are both enriched in the postsynaptic membrane at the NMJ in adult muscle (Fig. 5).

To investigate the basis of α-catulin synaptic localization, we electroporated tibialis anterior muscle with GFP-tagged truncation mutants of α-catulin domains called N, C1 and C2 (Fig. 6A) (Wiesner et al., 2008), and analyzed their subcellular localization. GFP alone was evenly distributed along the muscle fiber, in the cytoplasm and in nuclei (Fig. 6B). As expected, full-length GFP–α-catulin colocalized with AChRs at the NMJ (Fig. 6C–D,F–G). The N1+C1–GFP fusion was also concentrated at the NMJ (Fig. 6E) but, unlike the full-length protein, it failed to precisely localize within AChR-rich branches, forming small spicules (Fig. 6H,I) resembling those observed at the periphery of the postsynaptic machinery in α-dystrobrevin-KO mice (Grady et al., 2000). Neither of the α-catulin domains alone nor the C1+C2 fusion concentrated at the NMJ (Fig. 6J; data not shown). Thus, the N and C1 domains are required for localization of α-catulin to the NMJ, whereas the C2 domain is dispensable.

Immunohistochemical analysis of α-catulin and Grb2 in α-dystrobrevin-KO tissues demonstrated that, even in the absence of α-dystrobrevin, both proteins were still associated with postsynaptic membrane, although to a lower extent, as judged using the immunofluorescence intensity (Fig. S3A). This is in agreement with previous observations for α-catulin (Oh et al., 2012). Similar results were obtained after electroporation of GFP-fusion constructs into muscle tissues. Interestingly, in α-dystrobrevin-KO muscles, α-catulin localized additionally to muscle nuclei and the α-catulin NC1 construct was enriched predominantly around the nuclei (Fig. S3B). In contrast, we did not observe any nuclear localization for these proteins expressed in wild-type tissues. Also, Grb2 nuclear localization was more prominent in the knockout muscles. The second difference we observed was the striated pattern of α-catulin localization along the muscle fibers, which was observed only in the knockout muscles (Fig. S3B). The nature or importance of these differences needs further investigation.

α-Catulin is required for AChR cluster formation

To determine whether α-catulin is required for the formation of AChR clusters, we used small interfering (si)RNAs to deplete this protein from C2C12 myotubes. We differentiated myoblasts into myotubes on laminin-coated surfaces and transfected them with siRNAs that significantly affected expression of α-catulin, as verified by assaying mRNA and protein levels (Fig. 7A,B). As a positive control, we used an siRNA against MuSK, which we have previously shown blocks the formation of AChR clusters in this system (Proszynski and Sanes, 2013).

Untransfected myotubes formed numerous large clusters of complex topology, as well as small plaque-like AChR assemblies (Fig. 7C). In contrast, myotubes that had been depleted of α-catulin formed far fewer AChR clusters. The extent of the reduction was similar to that observed with siRNAs targeting MuSK (Fig. 7C,D). Three different siRNAs directed against α-catulin showed similar effects, whereas a variety of non-targeting control siRNAs had no effect (Fig. 7D; data not shown).

Grb2 is required for AChR cluster maturation

Finally, we assessed the roles of a phospho-dependent α-dystrobrevin-1 interacting protein, Grb2, on AChR clustering. We

Journal of Cell Science (2016) 129, 898-911 doi:10.1242/jcs.181180

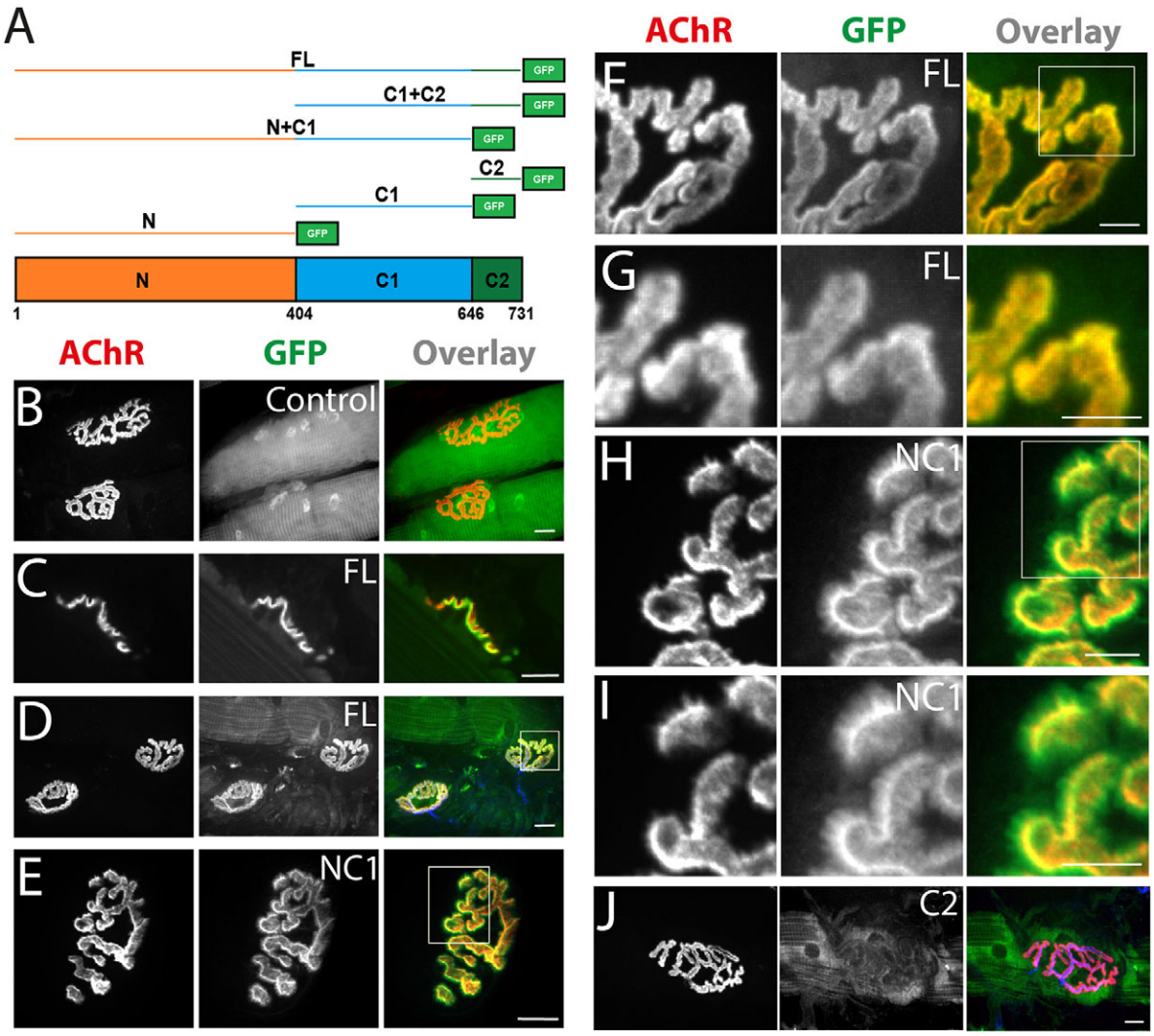

Fig. 6. Involvement of different α-catulin domains in the localization to the muscle postsynaptic machinery. (A) Schematic illustration of α-catulin domains and GFP fusion constructs used for electroporation (FL, full length; N, N-terminal domain; C1, amino acids 404–646 of the C-terminus; C2, amino acids 647–731 of the C-terminus). Numbers represent amino acids. (B–J) NMJ localization of constructs as indicated. (F,H) Higher magnification of areas boxed in D and E, respectively. (G,I) Higher magnification of areas boxed in F and H, respectively. Scale bars: 10 µm (B–E); 5 µm (F–J).

obtained three siRNAs that targeted Grb2 and decreased Grb2 mRNA and protein levels in C2C12 cells (Fig. 8A,B). Depletion of Grb2 with any of these effective siRNAs had no detectable effect on the initial formation of AChR clusters, but the number of the large topologically complex clusters was significantly reduced (Fig. 8C, D). Although we cannot rule out the possibility that initial clustering requires low levels of residual Grb2, we suggest that α-catulin and Grb2 have distinct effects because they act at different steps of the clustering and remodeling process.

DISCUSSION

Initial studies on postsynaptic maturation have demonstrated a central role for the DGC in the maturation of the postsynaptic membrane of the NMJ. Subsequent studies have identified α-dystrobrevin as a crucial mediator of the synaptic effects of the DGC and then successively focused on the α-dystrobrevin-1 isoform, the C-terminal extension of α-dystrobrevin-1 and phosphorylation of tyrosine residues in the C-terminal region (Balasubramanian et al., 1998; Blake et al., 1996; Grady et al., 2003, 2000; Pawlikowski and Maimone, 2009; Schmidt et al., 2011). Here, we have extended this work in several ways. First, we assessed the roles of three individual phosphorylation sites on maturation of the AChR clusters in cultured myotubes. Second, we generated and used phospho-specific antibodies to document dynamic regulation of α-dystrobrevin-1 phosphorylation *in vivo*. Third, we used biochemical methods to newly identify binding partners of α-dystrobrevin-1. These include liprin-α1, Usp9x and α-catulin as phospho-independent interactors, and Grb2, Arhgef5, PI3K, SH3BP2 and Fyn as phospho-dependent interactors. Finally, we demonstrated that α-catulin and Grb2 localize to the NMJ *in vivo*, and play a role in AChR clustering *in vitro*. Taken together, our results provide novel insight into α-dystrobrevin-1 function during the regulation of the postsynaptic specialization.

Having demonstrated that phosphorylation of residue Y713 is essential for α-dystrobrevin-1 function, we analyzed phosphorylation of this site at NMJs *in vivo*. We found that α-dystrobrevin-1 phosphorylation is regulated in two ways. First, levels of phospho-Y713 α-dystrobrevin-1 increase dramatically during the first two postnatal weeks, corresponding to the time when NMJs approach their adult size and remodel from plaque-shaped aggregates to

Journal of Cell Science (2016) 129, 898-911 doi:10.1242/jcs.181180

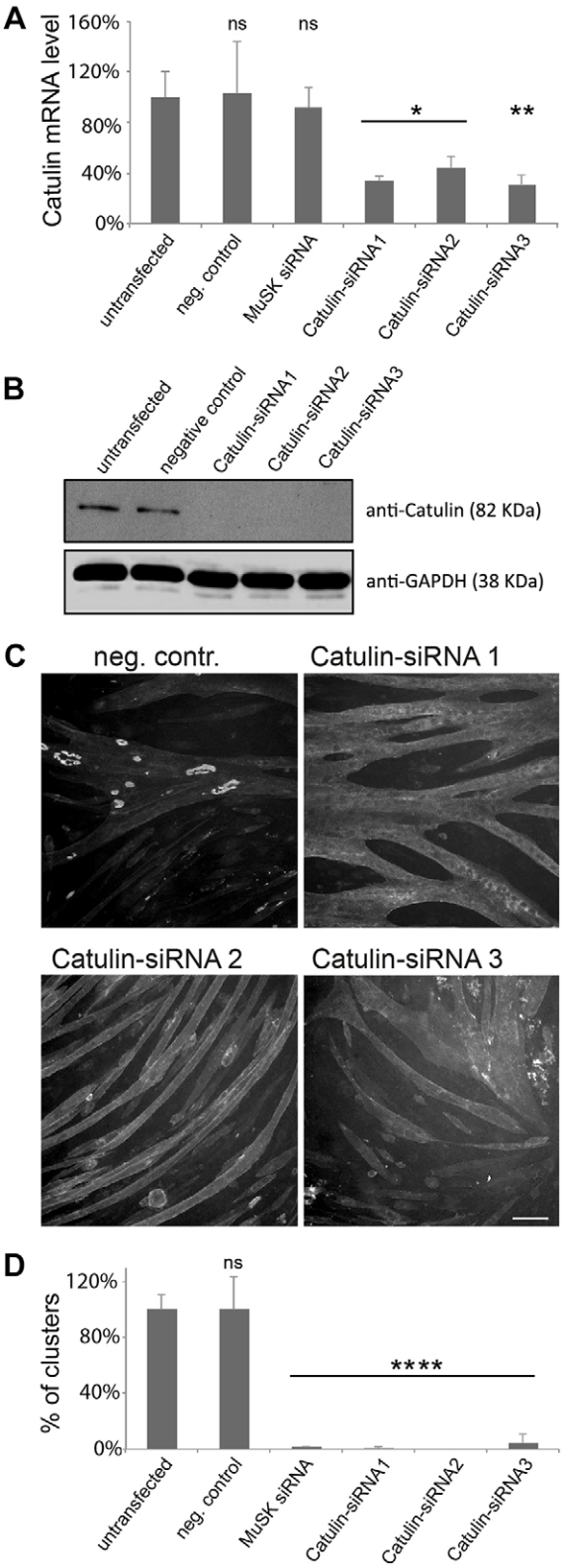

Fig. 7. α-Catulin plays a crucial role in the formation of AChR clusters. Different siRNAs were evaluated for their ability to deplete α-catulin expression by using RT-qPCR (A) and immunoblotting (B). Error bars represent s.d. ns, not significant. (C) Knockdown of α-catulin blocks the formation of AChR clusters. Laminin-cultured C2C12 myotubes were transfected with the siRNAs against the indicated genes and stained with α-bungarotoxin to visualize AChRs; scale bar: 50 µm. (D) Quantification of the number of clusters per visual field in myotubes transfected with the indicated siRNAs. The percentage of clusters (normalized to that in control) is shown as an average from three independent experiments; the number of complex clusters was *n*=158 for untransfected control, *n*=158 for negative control, *n*=2 for positive control, *n*=1 for α-catulin siRNA 1, *n*=0 for siRNA 2, *n*=7 for siRNA 3. Two-tailed Student *t*-test, mean± s.d., **P*<0.05, ***P*<0.01, *****P*<0.0001. neg. contr., negative control, non-targeting siRNA; MuSK siRNA, positive control.

topologically complex branched arrays. Second, levels of phospho-Y713 α-dystrobrevin-1 fall precipitously following denervation of adult muscle, and then return to control levels following reinnervation. These changes were unaccompanied by corresponding changes in α-dystrobrevin-1 immunoreactivity, as assessed with phospho-independent antibodies, indicating that it is phosphorylation rather than the level of α-dystrobrevin-1 that is subject to regulation. The effects of denervation and reinnervation provide strong evidence that α-dystrobrevin-1 phosphorylation is neurally regulated. Further experiments will be required to determine whether innervation affects phosphorylation by eliciting electrical activity or through the secretion of signaling molecules. Likewise, either increased nerve-evoked activity or enhanced secretion of a nerve-derived factor could account for the increased phosphorylation observed during the early postnatal period. One likely candidate secreted factor is neuregulin, which stimulates α-dystrobrevin-1 phosphorylation upon binding to its receptor, ErbB (Schmidt et al., 2011). ErbB is a tyrosine kinase; it might directly phosphorylate α-dystrobrevin-1 or stimulate phosphorylation indirectly by activating other kinases such as Src (Kuramochi et al., 2006; Ren et al., 2006; Vadlamudi et al., 2003). The latter possibility is supported by our finding that ectopic expression of a dominant-active Src mutant stimulates α-dystrobrevin-1 phosphorylation in HEK293 cells and the finding that Src phosphorylates purified α-dystrobrevin-1 *in vitro* (Balasubramanian et al., 1998). It is also possible that more than one kinase modifies α-dystrobrevin-1, and it would be beneficial to identify which kinase plays this role in various physiological and pathological processes *in vivo*.

Whatever their cause, alterations in α-dystrobrevin-1 phosphorylation could help to explain developmentally regulated and nerve-dependent alterations in the postsynaptic membrane. During early postnatal life, AChR aggregates remodel, and AChR half-life in the membrane increases. Following denervation, AChR levels and stability both decrease (Loring and Salpeter, 1980). Our previous studies have demonstrated that NMJs in α-dystrobrevin-mutant mice exhibit decreased AChR levels, increased AChR turnover time and morphological alterations (Grady et al., 2000), and others have shown that AChR clusters in α-dystrobrevin-deficient myotubes fail to acquire complex morphologies (Pawlikowski and Maimone, 2009). We have also shown that these defects can be rescued by reintroduction of α-dystrobrevin-1 but not by nonphosphorylatable mutants of α-dystrobrevin-1. The remaining question was whether levels of α-dystrobrevin-1 phosphorylation are in fact modulated during development and by innervation. We have now shown that they are. A reasonable inference, then, is that alterations in the phosphorylation of α-dystrobrevin-1 influence its ability to mediate postsynaptic maturation and stability.

How might the α-dystrobrevin-1 interactors that we have identified help to mediate the effects of α-dystrobrevin-1? Clues come from studies on the function and localization of these proteins. First, Grb2, Arhgef5 and PI3K, which all interact with phospho-α-dystrobrevin-1, form a complex that initiates the formation of podosomes – membrane-associated organelles implicated in adhesion and ECM remodeling (Kuroiwa et al., 2011; Murphy and

Journal of Cell Science (2016) 129, 898-911 doi:10.1242/jcs.181180

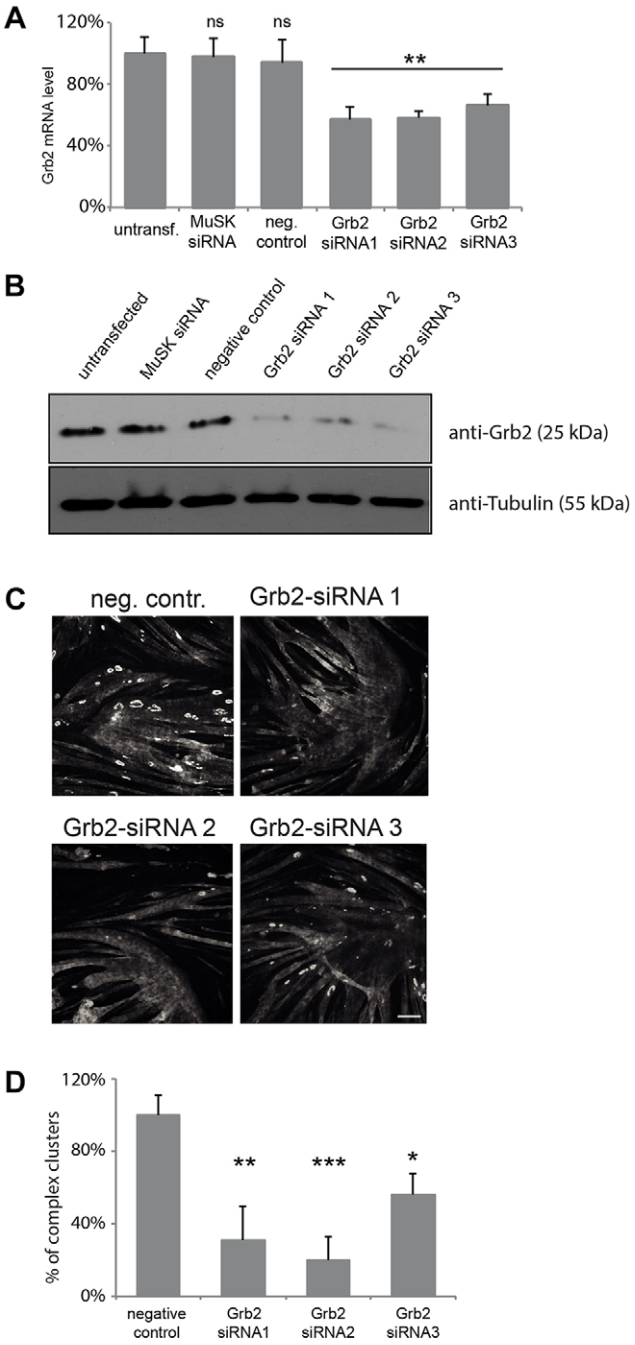

Fig. 8. Grb2 is required for the formation of complex AChR clusters. Different siRNAs were evaluated for their ability to deplete Grb2 expression by using RT-qPCR (A) and immunoblotting (B). Error bars represent s.d. (C) Knockdown of Grb2 affects the formation of large AChR clusters with complex topology. Laminin-cultured C2C12 myotubes were transfected with siRNAs against the indicated genes and stained with α-bungarotoxin to visualize AChRs. Scale bar: 50 µm. (D) Quantification of the number of complex clusters per visual field in control and Grb2-depleted myotubes. The percentage of clusters (normalized to control) is shown as an average from three independent experiments; the number of clusters was n=343 for negative control, n=76 for siRNA 1, n=49 for siRNA 2 and n=110 for siRNA 3. Two-tailed Student t-test; mean±s.e.m.; *P<0.05, **P<0.01, ***P<0.001; ns, not significant; neg. contr., negative control, non-targeting siRNA; MuSK siRNA, positive control.

Courtneidge, 2011; Oikawa et al., 2008). We have previously shown that podosomes are involved in the remodeling of AChR clusters in cultured myotubes (Proszynski et al., 2009; Bernadzki et al., 2014). Additionally, liprin-α1, which binds both to α-dystrobrevin-1 and to α-catulin, has been implicated in the maturation of vertebrate central synapses (Spangler et al., 2011, 2013) and the *Drosophila* NMJ (Kaufmann et al., 2002). Moreover, liprin-α1 interacts with ELKS, which regulates synapses in the brain and is a component of AChR-rich aggregates in myotubes (Astro et al., 2011; Ko et al., 2003; Nomura et al., 2011; Owald et al., 2010; Proszynski and Sanes, 2013; Proszynski et al., 2009). Third, the protein-tyrosine kinase Fyn, identified here as a phospho-α-dystrobrevin-1-interacting protein, has been previously shown to be dispensable for AChR cluster formation but required for their stabilization (Smith et al., 2001). Finally, these interactors form multimolecular networks. For example, α-catulin, which is a general interactor for α-dystrobrevin-1 also binds to syntrophin, utrophin, β-dystrobrevin (a product of a different gene from that encoding α-dystrobrevin-1) and Arhgef5 (Lyssand et al., 2010). Our studies have identified that Arhgef5 is also a phospho-dependent α-dystrobrevin-1 ligand. Moreover, Grb2 binds to two other components of the DGC – syntrophin and dystroglycan (Oak et al., 2001; Yang et al., 1995); and Fyn interacts with AChRs, Grb2, PI3K and SH3BP2 (Foucault et al., 2005; Fuhrer and Hall, 1996; Gout et al., 1992; Kapeller et al., 1994; Li et al., 1996). Binding to multiple components is characteristic for proteins that have important functions in the organization of synaptic machinery and could explain α-catulin and Grb2 synaptic localization in α-dystrobrevin-KO tissues. This could account for the much stronger phenotype that is observed in α-catulin- and Grb2-depleted myotubes as compared to that of α-dystrobrevin-KO cells. Based on our observations, a picture emerges in which α-dystrobrevin-1 serves as a hub to assemble complexes of signaling proteins that impinge upon the organization of the postsynaptic machinery.

MATERIALS AND METHODS

Cell culture

C2C12 cells [American Type Culture Collection (ATCC); catalog number CRL-1772] were cultured for up to five passages in Dulbecco's modified Eagle's medium (DMEM) containing 20% fetal bovine serum supplemented with 4.5 g/l of glutamine, penicillin, streptomycin and Fungizone. Cells were trypsinized and replated onto 8-well Permanox chamber slides (Sigma-Aldrich; catalog number 177445). Before plating, slides were coated with 10 µg/ml solution of laminin 111 (Invitrogen; catalog number 23017–015) in L-15 medium supplemented with 0.2% $NaHCO_3$ or DMEM, incubated overnight at 37°C and aspirated immediately before plating cells. To induce cell fusion, growth medium was replaced with fusion medium containing 2% horse serum in DMEM supplemented with 4.5 g/l of glutamine, penicillin, streptomycin and Fungizone. Primary muscle cell culture was performed as described previously (Proszynski et al., 2009). Formation of AChR clusters in primary myotubes was analyzed by an investigator that was blind to the samples, and the cluster categories were confirmed by an independent investigator. HEK293 cells (ATCC; catalog number CRL-1573) were cultured in DMEM containing 10% fetal bovine serum supplemented with glutamine, penicillin, streptomycin and Fungizone. Transient transfections of HEK293 cells were performed with TransIT®-LT1 Transfection Reagent (Mirus Bio LLC; catalog number MIR 2300), according to the manufacturer's instructions. Where indicated, cells were incubated with 0.1 mM sodium orthovanadate with 0.003% hydrogen peroxide to inhibit phosphatases. The state and authenticity of all cells was carefully analyzed before performing experiments.

Immunofluorescence

Cultured cells were fixed with acetone or 1–4% paraformaldehyde, supplemented in some cases with 0.1% glutaraldehyde. Following fixation, cells were treated with sodium borohydride for 3–5 min and washed with PBS. Before overnight incubation with primary antibodies, nonspecific staining was blocked with 2% BSA and 2% goat serum in PBS with 0.1% Triton X-100.

Journal of Cell Science (2016) 129, 898-911 doi:10.1242/jcs.181180

Muscles from wild-type and α-dystrobrevin-1-KO animals were fixed in 2% paraformaldehyde, rinsed in PBS, cryoprotected in 30% sucrose at 4°C and sectioned at 4–10 µm in a cryostat. For staining for phospho-α-dystrobrevin-1 (see below), muscles were superfused with pervanadate (0.1 mM sodium orthovanadate with 0.003% hydrogen peroxide) for 10 min prior to dissection and fixation. For whole-mount staining, muscles were briefly fixed in cold methanol and washed with PBS. Nonspecific staining was blocked with 2% BSA and 2% goat serum in PBS plus 0.1% Triton X-100 before overnight incubation with primary antibodies.

Sources of primary antibodies were as follows (catalog numbers given in brackets): rabbit anti-catulin (GTX112226; dilution 1:300), anti-liprin (GTX115098; dilution 1:300) and anti-Fyn (GTX101189; dilution 1:500) antibodies were from GeneTex (Irvine, CA); rabbit anti-Grb2 (1584-1 and 1517-1; dilutions 1:500), anti-p85 (1675-1; dilution 1:500), anti-α-catulin (S2478; dilution 1:500) and anti-GFP (1533-1; dilution 1:1000) antibodies were from Epitomics (Burlingame, CA); mouse anti-Usp9x (AT4497a; dilution 1:500) antibody was from Abgent (San Diego, CA); rabbit and mouse anti-GFP antibodies (JM-3999-100 and A-11120, respectively; dilutions 1:500) were from MBL (Woburn, MA, USA) and Invitrogen (Grand Island, NY, USA), respectively; mouse antibody against pan-phospho-tyrosine residues (610000; dilution 1:500) and the rabbit anti-α-dystrobrevin-1 antibody were generated in the Sanes laboratory (DB692; dilution 1:1000); the anti-α-dystrobrevin-2 antibody was a gift from Professor Stan C. Froehner (University of Washington, Seattle, WA) and the mouse antibody against all isoforms of α-dystrobrevin (610766; dilution 1:500) was from BD Transduction Lab (Franklin Lakes, NJ); mouse anti-GST (71097-3; dilution 1:500) and anti-GAPDH (MAB374; dilution 1:500) antibodies were from Millipore; mouse anti-His antibody (A00186-100; dilution 1:500) was from Genescript (Piscataway, NJ); rabbit anti-tubulin antibody (ab18251; dilution 1:1000) was from Abcam (Cambridge, UK); rabbit anti-liprin antibody (Asperti et al., 2009) (dilution 1:500) was a gift from Dr Ivan de Curtis (San Raffaele University and San Raffaele Scientific Institute, Milan, Italy). Phalloidin, used to visualize F-actin, was conjugated to Alexa-Fluor-488 or -568 (Invitrogen). AChRs were labeled with α-bungarotoxin conjugated to Alexa-Fluor-488 or -555 (Invitrogen). Primary antibodies were detected with Alexa-Fluor-488, -568 or -647-coupled goat secondary antibodies (Invitrogen).

To generate phospho-specific antibodies to α-dystrobrevin-1, rabbits were immunized with synthetic phosphopeptides (Y713: N′-CTQPEDGNpYENESVR-C′; Y730: N′-CNELQLEEpYLKQKLQD-C′, where 'p' indicates phosphorylation of the proceeding tyrosine residue), and antisera were purified by positive and negative selection on phosphorylated and non-phosphorylated peptides, respectively (Covance, Dedham, MA, USA).

Microscopy

Epifluorescence images of fixed cells were collected on an Axio Imager Z1 microscope (Carl Zeiss) fitted with a cooled charge-coupled device (CCD) camera and PLAN-NEO FLUAR 40×/1.3 oil objective, or a Nikon ECLIPSE TE 2000-E microscope equipped with a Hamamatsu 1394 ORCA-ERA camera (Hamamatsu Photonics) and PLAN APO 40×/0.95 DIC M/N2 objective. Confocal images were obtained using Fluoview1000 equipped with 40×, 1.3 NA objective lenses. Images were analyzed with NIS-Elements AR 3.0 software (Nikon) and edited with Adobe Photoshop version 8.0.

DNA constructs

eGFP–αDB1 (either WT or Y/F) was fused to the TAP epitope tags as follows. Sequences encoding a TAP epitope tag, comprising Protein A, a Tobacco Etch Virus (TEV) protease cleavage site and StrepII tag were excised from plasmid pTetp-N-Pts (Giannone et al., 2007), a gift from Yisong Wang (Oak Ridge National Laboratory, Tennessee). It was inserted into the pShuttle-CMV plasmid, along with the sequence encoding eGFP–αDB1 (Grady et al., 2003). The resulting plasmids, pShuttle-CMV-TAP-eGFP-αDB1(WT) and pShuttle-CMV-TAP-eGFP-αDB1(Y/F) were used to produce recombinant adenovirus using AdEasy system (He et al., 1998). Plasmids containing dominant-active and dominant-negative mutants of Src (Addgene entry 13660 and 13657, respectively) and wild-type Fyn [Addgene entry 16032; (Mariotti et al., 2001)] were obtained from Addgene (Cambridge, MA, USA). Mouse α-catulin full-length and truncation mutant cDNAs were PCR amplified and cloned into pcDNA3.1-puro-C′GFP expression vector with the following sets of primers: Forward 1: 5′-CTGGA**GGCCGGC**CATGGCCGCTTCTCCAGTCCCGG-3′ (1–22 bp), Reverse 1: 5′-CTTCT**GAATTC**AGCTGCATGGCTGTACAATGGAGTTC-3′ (1183–1208 bp), Forward 2: 5′-CTGGA**GGCCGGCC**ATGGCAGCCGACCTGTTAAAATTC-3′ (1210–1230 bp), Reverse 2: 5′-CTTCT**GAATTC**TGTTTTGAAAATGACTGTACAC-3′ (1916–1937 bp), Forward 3: 5′-CTGGA**GGCCGGCC**ATGCTAAAAGATGATGACAAAC-3′ (1939–1957 bp), Reverse 3: 5′-CTTCT**GAATTC**CAGTTTTGACCATCCATGGTATC-3′ (2173–2195 bp). Bases in bold represent the sequences recognized by restriction enzymes. The ranges given in brackets represent the positions in the cDNA.

Mouse Grb2 cDNA was PCR amplified and cloned into pcDNA3.1-puro-N′GFP expression vector with the following set of primers: Forward 1: 5′-CTGGA**GAATTC**ATGGAAGCCATCGCCAAATATGAC-3′ (1–24 bp), Reverse 1: 5′-GTATC**GATATC**GACGTTCCGGTTCACGGGGGTGACATAATTGC-3′ (620–651 bp).

Complex purification and mass spectrometry analysis

Adenoviral particles were produced by Welgen (Worcester, MA) from a vector encoding TAP–αDB1(WT) and TAP-αDB1(3×Y/F). C2C12 myotubes were infected with adenovirus on the second day after fusion induction. Two days later, the myotubes were treated with pervanadate (0.1 mM sodium orthovanadate with 0.003% hydrogen peroxide), washed with ice-cold PBS containing sodium azide and covered with lysis buffer [50 mM Tris-HCl, 150 mM NaCl, 50 mM NaH_2PO_4, 10 mM imidazole, 0.1% Nonidet-P40, 10% glycerol, 10 mM β-mercaptoethanol, EDTA-free mini protease inhibitor cocktail (Roche), 1 mM phenylmethylsulphonyl fluoride, pervanadate, pH 8.0]. Cells were scraped off the dish, incubated briefly on ice, passed three times through a 25-gauge needle with syringe and centrifuged for 5 min at 4000 ***g*** and 30 min at 21,000 ***g***. The supernatant was incubated with washed IgG Sepharose 6 Fast Flow from GE Healthcare (catalog number 17-0969-01) for 4–16 h. Next, the Sepharose was loaded into a column (Bio-Rad; catalog number 731-1550), washed three times with wash buffer (50 mM Tris-HCl, 50 mM NaH_2PO_4, 150 mM NaCl, 0.1% NP-40, pervanadate, pH 8.0), washed once with TEV buffer (50 mM Tris-HCl, 150 mM NaCl, 0.5 mM EDTA, 1 mM DTT, pervanadate, pH 8.0) and resuspended in TEV buffer. To cleave the protein from the Sepharose, AcTEV (Invitrogen; catalog number 12575-015) was added, and the sample was incubated for 2 h at room temperature or overnight at 4°C. For precipitation of proteins from eluted samples, 25% of the sample volume of 100% trichloroacetic acid (TCA) (500 g of TCA in 350 ml of H_2O) was added, incubated for 10 min at 4°C and centrifuged at 18,000 ***g*** for 5 min. The pellet was washed with 200 µl of cold acetone, centrifuged at 18,000 ***g*** for 5 min, air dried and resuspended in sample buffer followed by incubation at 95°C for 6 min.

Peptide-based protein purification was performed essentially as described previously (Hallock et al., 2010). Synthetic peptides (phospho-Y713: DEST–Biotin–Ahx–TQPEDGNp**Y**ENESVRQ-NH_2, Y713: DEST–Biotin–Ahx–TQPEDGN**Y**ENESVRQ-NH_2, phospho-Y730: DEST– Biotin–Ahx–RQLENELQLEEp**Y**LKQKLQDE-NH_2 and Y730: DEST–Biotin– Ahx–RQLENELQLEE**Y**LKQKLQDE-NH_2; NH_2 denotes peptide amidation, and 'p' indicates phosphorylation of the proceeding tyrosine residue) were produced by Lifetein (South Plainfield, NJ). Residues in bold represent the tyrosine residue of interest. Peptides (40 µg each) were attached to Dynabeads M-280 (catalog number 11205D) obtained from Invitrogen. Beads, after washing four times with PBS and once with lysis buffer, were incubated with cell lysate (see above). After incubation, beads were washed four times with lysis buffer and boiled in sample buffer for 5 min. For analysis, samples were subjected to SDS-PAGE, and proteins were visualized with SilverQuest (Invitrogen; catalog number LC6070). Gels were stained with Colloidal Blue Staining Kit (Invitrogen; catalog LC6025). Slices were excised from the gel and analyzed at the Harvard Microchemistry and Proteomics Analysis Facility by using µLC-MS-MS on a Thermo LTQ-Orbitrap mass spectrometer.

Journal of Cell Science (2016) 129, 898-911 doi:10.1242/jcs.181180

Immunoprecipitation

HEK293 cells were transfected with appropriate constructs and lysed as described above for myotubes. Lysates were centrifuged, and supernatants were incubated for 2 h to overnight with Dynabeads from Invitrogen coated with anti-GFP antibody. Beads were then washed four times with lysis buffer, resuspended in 2× sample buffer and boiled for 5 min. For western blotting analysis, samples were loaded on pre-cast gels from Bio-Rad (Hercules; catalog number 456-1086), subjected to the SDS-PAGE and transferred to the Immobilon-P membrane from Millipore (Billerica; catalog number IPVH00010). For pulldown experiments, Dynabeads M-280 (11205D) from Invitrogen were coated with biotinylated synthetic peptides (see above), incubated with recombinant proteins in HEPES buffer [20 mM HEPES, 150 mM NaCl, 0.5 mM EDTA, 10% glycerol, 0.05% NP-40, 1 mM DTT, EDTA-free Mini protease inhibitor cocktail (Roche), 1 mM phenylmethylsulphonyl fluoride, pervanadate, pH 7.9]. Subsequently, beads were washed four times with HEPES buffer and boiled in sample buffer. Recovery of recombinant proteins was evaluated by western blotting.

Alternatively, Dynabeads M-280 were coated with purified GFP–αDB1 constructs (either WT or 3×Y/F) expressed in HEK293. For this, HEK293 cells were transfected with either a GFP–αDB1 plasmid or co-transfected together with plasmid expressing the indicated Src mutant (induction of α-dystrobrevin-1 phosphorylation). Before lysing, cells were treated (if indicated) with pervanadate for 10 min and lysed in RIPA buffer (catalog number R0278) from Sigma-Aldrich supplemented with 0.6 M NaCl. After four subsequent washes with the RIPA buffer, beads were washed two more times in HEPES buffer (see above) and incubated with indicated recombinant protein. After incubation, beads were washed four times with HEPES buffer and boiled in sample buffer. Recovery of recombinant proteins was evaluated by western blotting analysis. Full-length PI3K (p110α+p85α; catalog number P27-18H) and Grb2 (catalog number G45-30G-50) were obtained from SignalChem (Richmond, BC, Canada).

Animals

α-dystrobrevin-1 mutants were generated and genotyped as described previously by Grady et al. (1999) and maintained on a C57B6 background (Grady et al., 1999). Wild-type C57B6 mice were obtained from Jackson Laboratories. Experiments were performed on mice at P30 (unless indicated differently in the figure legend) of either sex, and according to protocols approved by both the Harvard University Standing Committee on the Use of Animals in Research and Teaching, and the First Warsaw Local Ethics Committee for Animal Experimentation at the Nencki Institute.

Denervation of the sternomastoid muscle was performed by cutting or crushing the accessory nerve, as described previously by Rich and Lichtman (1989). Briefly, under aseptic conditions, a midline incision was made in the neck, and the salivary glands were retracted to expose the right sternomastoid muscle. For permanent denervation, a 2- to 3-mm-long segment of nerve was cut out and removed. For transient denervation, the nerve was crushed with forceps near the entry point into the tibia. The wound was closed, and the animal was allowed to recover. Confirmation of cut or crush was assessed by immunostaining the nerve and presynaptic nerve terminals upon tissue collection.

Electroporation of tibialis anterior muscle of 1-month-old mice was performed as previously described (McMahon et al., 2001), and muscles were extracted 3 weeks after electroporation.

Knockdown experiments and quantitative PCR analysis

For gene knockdown in C2C12 myotubes, cells were transfected with 20 nM siRNA using Lipofectamine RNAiMAX (Invitrogen) at 48–72 h after fusion and fixed 3 days later. For α-catulin silencing, the following siRNAs were used: siRNA1 SI00942032, siRNA2 SI00942011 and siRNA3 SI00942018; and for silencing of Grb2, the following siRNAs were used: siRNA1 SI02667168, siRNA2 SI04060126 and siRNA3 SI02732884 (Qiagen). Non-targeting siRNA-B was purchased from Santa Cruz (catalog number sc-44230). MuSK siRNA was as used previously (Proszynski and Sanes, 2013). Real-time quantitative (RT-q)PCR analysis was performed at least in duplicates for RNAs obtained from three independent experiments. RNA was isolated from myotubes using the Trisure Reagent (Bioline) according to the manufacturer's instructions. To visualize RNA pellets, 5–10 µg of glycogen (Invitrogen) was added to the samples. cDNA was generated from 0.5–2 µg of templates using the High-Capacity cDNAReverse Transcription Kit (Applied Biosystems, Life Tech). RT-qPCR was performed using Fast SYBR Green Master Mix (Applied Biosystems, Life Tech) on the Step One Plus instrument (Applied Biosystems, Life Tech). Results were analyzed with StepOne software v.2.3 using the standard curve method and standardized to GAPDH as the housekeeping gene. Statistical analysis was performed using a two-tailed *t*-test.

Acknowledgements

We thank the Harvard Microchemistry and Proteomics Facility for performing mass spectrometry.

Competing interests

The authors declare no competing or financial interests.

Author contributions

J.G., M.G., K.M.B., R.M.G., P.H. and T.J.P. performed experiments; T.J.P., J.R.S. and J.G. wrote the manuscript; J.G., M.G., K.M.B., R.M.G., P.H., D.J.G., J.R.S. and T.J.P. planned experiments and analyzed data.

Funding

This work was supported by the grants from the National Institutes of Health – National Institute of Neurological Disorders and Stroke [grant numbers NS59853 and NS19195 to J.R.S.], as well as by a grant from the Polish National Science Center (NCN) [grant number 2013/09/B/NZ3/03524 to T.J.P.]. The project was performed with the use of CePT infrastructure financed by the European Union – the European Regional Development Fund within the Operational Program 'Innovative Economy' for 2007–2013. Deposited in PMC for release after 12 months.

Supplementary information

Supplementary information available online at
http://jcs.biologists.org/lookup/suppl/doi:10.1242/jcs.181180/-/DC1

References

Acebes, A. and Morales, M. (2012). At a PI3K crossroads: lessons from flies and rodents. *Rev. Neurosci.* **23**, 29-37.

Asperti, C., Astro, V., Totaro, A., Paris, S. and de Curtis, I. (2009). Liprin-alpha1 promotes cell spreading on the extracellular matrix by affecting the distribution of activated integrins. *J. Cell Sci.* **122**, 3225-3232.

Astro, V., Asperti, C., Cangi, M. G., Doglioni, C. and de Curtis, I. (2011). Liprin-alpha1 regulates breast cancer cell invasion by affecting cell motility, invadopodia and extracellular matrix degradation. *Oncogene* **30**, 1841-1849.

Balasubramanian, S., Fung, E. T. and Huganir, R. L. (1998). Characterization of the tyrosine phosphorylation and distribution of dystrobrevin isoforms. *FEBS Lett.* **432**, 133-140.

Bernadzki, K. M., Rojek, K. O. and Proszynski, T. J. (2014). Podosomes in muscle cells and their role in the remodeling of neuromuscular postsynaptic machinery. *Eur. J. Cell Biol.* **93**, 478-485.

Blake, D. J., Nawrotzki, R., Peters, M. F., Froehner, S. C. and Davies, K. E. (1996). Isoform diversity of dystrobrevin, the murine 87-kDa postsynaptic protein. *J. Biol. Chem.* **271**, 7802-7810.

Brown, R. H., Jr. (1997). Dystrophin-associated proteins and the muscular dystrophies. *Annu. Rev. Med.* **48**, 457-466.

Choi, H. Y., Liu, Y., Tennert, C., Sugiura, Y., Karakatsani, A., Kröger, S., Johnson, E. B., Hammer, R. E., Lin, W. and Herz, J. (2013). APP interacts with LRP4 and agrin to coordinate the development of the neuromuscular junction in mice. *eLife* **2**, e00220.

Cougoule, C., Le Cabec, V., Poincloux, R., Al Saati, T., Mege, J.-L., Tabouret, G., Lowell, C. A., Laviolette-Malirat, N. and Maridonneau-Parini, I. (2010). Three-dimensional migration of macrophages requires Hck for podosome organization and extracellular matrix proteolysis. *Blood* **115**, 1444-1452.

Darabid, H., Perez-Gonzalez, A. P. and Robitaille, R. (2014). Neuromuscular synaptogenesis: coordinating partners with multiple functions. *Nat. Rev. Neurosci.* **15**, 703-718.

Ervasti, J. M. and Campbell, K. P. (1993). A role for the dystrophin-glycoprotein complex as a transmembrane linker between laminin and actin. *J. Cell Biol.* **122**, 809-823.

Foucault, I., Le Bras, S., Charvet, C., Moon, C., Altman, A. and Deckert, M. (2005). The adaptor protein 3BP2 associates with VAV guanine nucleotide exchange factors to regulate NFAT activation by the B-cell antigen receptor. *Blood* **105**, 1106-1113.

Fuhrer, C. and Hall, Z. W. (1996). Functional interaction of Src family kinases with the acetylcholine receptor in C2 myotubes. *J. Biol. Chem.* **271**, 32474-32481.
Giannone, R. J., McDonald, W. H., Hurst, G. B., Huang, Y., Wu, J., Liu, Y. and Wang, Y. (2007). Dual-tagging system for the affinity purification of mammalian protein complexes. *Biotechniques* **43**, 296-302.
Giubellino, A., Burke, T. R., Jr. and Bottaro, D. P. (2008). Grb2 signaling in cell motility and cancer. *Expert Opin. Ther. Targets* **12**, 1021-1033.
Gout, I., Dhand, R., Panayotou, G., Fry, M. J., Hiles, I., Otsu, M. and Waterfield, M. D. (1992). Expression and characterization of the p85 subunit of the phosphatidylinositol 3-kinase complex and a related p85 beta protein by using the baculovirus expression system. *Biochem. J.* **288**, 395-405.
Grady, R. M., Grange, R. W., Lau, K. S., Maimone, M. M., Nichol, M. C., Stull, J. T. and Sanes, J. R. (1999). Role for alpha-dystrobrevin in the pathogenesis of dystrophin-dependent muscular dystrophies. *Nat. Cell Biol.* **1**, 215-220.
Grady, R. M., Zhou, H., Cunningham, J. M., Henry, M. D., Campbell, K. P. and Sanes, J. R. (2000). Maturation and maintenance of the neuromuscular synapse: genetic evidence for roles of the dystrophin–glycoprotein complex. *Neuron* **25**, 279-293.
Grady, R. M., Akaaboune, M., Cohen, A. L., Maimone, M. M., Lichtman, J. W. and Sanes, J. R. (2003). Tyrosine-phosphorylated and nonphosphorylated isoforms of alpha-dystrobrevin: roles in skeletal muscle and its neuromuscular and myotendinous junctions. *J. Cell Biol.* **160**, 741-752.
Greer, P. (2002). Closing in on the biological functions of Fps/Fes and Fer. *Nat. Rev. Mol. Cell Biol.* **3**, 278-289.
Hallock, P. T., Xu, C.-F., Park, T.-J., Neubert, T. A., Curran, T. and Burden, S. J. (2010). Dok-7 regulates neuromuscular synapse formation by recruiting Crk and Crk-L. *Genes Dev.* **24**, 2451-2461.
He, T.-C., Zhou, S., da Costa, L. T., Yu, J., Kinzler, K. W. and Vogelstein, B. (1998). A simplified system for generating recombinant adenoviruses. *Proc. Natl. Acad. Sci. USA* **95**, 2509-2514.
Jacobson, C., Côté, P. D., Rossi, S. G., Rotundo, R. L. and Carbonetto, S. (2001). The dystroglycan complex is necessary for stabilization of acetylcholine receptor clusters at neuromuscular junctions and formation of the synaptic basement membrane. *J. Cell Biol.* **152**, 435-450.
Kapeller, R., Prasad, K. V., Janssen, O., Hou, W., Schaffhausen, B. S., Rudd, C. E. and Cantley, L. C. (1994). Identification of two SH3-binding motifs in the regulatory subunit of phosphatidylinositol 3-kinase. *J. Biol. Chem.* **269**, 1927-1933.
Kaufmann, N., DeProto, J., Ranjan, R., Wan, H. and Van Vactor, D. (2002). Drosophila liprin-alpha and the receptor phosphatase Dlar control synapse morphogenesis. *Neuron* **34**, 27-38.
Ko, J., Na, M., Kim, S., Lee, J.-R. and Kim, E. (2003). Interaction of the ERC family of RIM-binding proteins with the liprin-alpha family of multidomain proteins. *J. Biol. Chem.* **278**, 42377-42385.
Kummer, T. T., Misgeld, T., Lichtman, J. W. and Sanes, J. R. (2004). Nerve-independent formation of a topologically complex postsynaptic apparatus. *J. Cell Biol.* **164**, 1077-1087.
Kuramochi, Y., Guo, X. and Sawyer, D. B. (2006). Neuregulin activates erbB2-dependent src/FAK signaling and cytoskeletal remodeling in isolated adult rat cardiac myocytes. *J. Mol. Cell. Cardiol.* **41**, 228-235.
Kuroiwa, M., Oneyama, C., Nada, S. and Okada, M. (2011). The guanine nucleotide exchange factor Arhgef5 plays crucial roles in Src-induced podosome formation. *J. Cell Sci.* **124**, 1726-1738.
Li, B., Subleski, M., Fusaki, N., Yamamoto, T., Copeland, T., Princler, G. L., Kung, H. and Kamata, T. (1996). Catalytic activity of the mouse guanine nucleotide exchanger mSOS is activated by Fyn tyrosine protein kinase and the T-cell antigen receptor in T cells. *Proc. Natl. Acad. Sci. USA* **93**, 1001-1005.
Loring, R. H. and Salpeter, M. M. (1980). Denervation increases turnover rate of junctional acetylcholine receptors. *Proc. Natl. Acad. Sci. USA* **77**, 2293-2297.
Lyssand, J. S., Whiting, J. L., Lee, K.-S., Kastl, R., Wacker, J. L., Bruchas, M. R., Miyatake, M., Langeberg, L. K., Chavkin, C., Scott, J. D. et al. (2010). Alpha-dystrobrevin-1 recruits alpha-catulin to the alpha1D-adrenergic receptor/dystrophin-associated protein complex signalosome. *Proc. Natl. Acad. Sci. USA* **107**, 21854-21859.
Mariotti, A., Kedeshian, P. A., Dans, M., Curatola, A. M., Gagnoux-Palacios, L. and Giancotti, F. G. (2001). EGF-R signaling through Fyn kinase disrupts the function of integrin alpha6beta4 at hemidesmosomes: role in epithelial cell migration and carcinoma invasion. *J. Cell Biol.* **155**, 447-458.
McMahon, J. M., Signori, E., Wells, K. E., Fazio, V. M. and Wells, D. J. (2001). Optimisation of electrotransfer of plasmid into skeletal muscle by pretreatment with hyaluronidase – increased expression with reduced muscle damage. *Gene Ther.* **8**, 1264-1270.
Murphy, D. A. and Courtneidge, S. A. (2011). The 'ins' and 'outs' of podosomes and invadopodia: characteristics, formation and function. *Nat. Rev. Mol. Cell Biol.* **12**, 413-426.
Newey, S. E., Gramolini, A. O., Wu, J., Holzfeind, P., Jasmin, B. J., Davies, K. E. and Blake, D. J. (2001). A novel mechanism for modulating synaptic gene expression: differential localization of alpha-dystrobrevin transcripts in skeletal muscle. *Mol. Cell Neurosci.* **17**, 127-140.
Nomura, H., Tadokoro, S. and Hirashima, N. (2011). Liprin-alpha is involved in exocytosis and cell spreading in mast cells. *Immunol. Lett.* **139**, 110-116.
Oak, S. A., Russo, K., Petrucci, T. C. and Jarrett, H. W. (2001). Mouse alpha1-syntrophin binding to Grb2: further evidence of a role for syntrophin in cell signaling. *Biochemistry* **40**, 11270-11278.
Oh, H. J., Abraham, L. S., van Hengel, J., Stove, C., Proszynski, T. J., Gevaert, K., DiMario, J. X., Sanes, J. R., van Roy, F. and Kim, H. (2012). Interaction of alpha-catulin with dystrobrevin contributes to integrity of dystrophin complex in muscle. *J. Biol. Chem.* **287**, 21717-21728.
Oikawa, T., Itoh, T. and Takenawa, T. (2008). Sequential signals toward podosome formation in NIH-src cells. *J. Cell Biol.* **182**, 157-169.
Owald, D., Fouquet, W., Schmidt, M., Wichmann, C., Mertel, S., Depner, H., Christiansen, F., Zube, C., Quentin, C., Korner, J. et al. (2010). A Syd-1 homologue regulates pre- and postsynaptic maturation in Drosophila. *J. Cell Biol.* **188**, 565-579.
Pawlikowski, B. T. and Maimone, M. M. (2009). Formation of complex AChR aggregates in vitro requires alpha-dystrobrevin. *Dev. Neurobiol.* **69**, 326-338.
Peters, M. F., Adams, M. E. and Froehner, S. C. (1997). Differential association of syntrophin pairs with the dystrophin complex. *J. Cell Biol.* **138**, 81-93.
Peters, M. F., Sadoulet-Puccio, H. M., Grady, M. R., Kramarcy, N. R., Kunkel, L. M., Sanes, J. R., Sealock, R. and Froehner, S. C. (1998). Differential membrane localization and intermolecular associations of alpha-dystrobrevin isoforms in skeletal muscle. *J. Cell Biol.* **142**, 1269-1278.
Proszynski, T. J. and Sanes, J. R. (2013). Amotl2 interacts with LL5beta, localizes to podosomes and regulates postsynaptic differentiation in muscle. *J. Cell Sci.* **126**, 2225-2235.
Proszynski, T. J., Gingras, J., Valdez, G., Krzewski, K. and Sanes, J. R. (2009). Podosomes are present in a postsynaptic apparatus and participate in its maturation. *Proc. Natl. Acad. Sci. USA* **106**, 18373-18378.
Reichenberger, E. J., Levine, M. A., Olsen, B. R., Papadaki, M. E. and Lietman, S. A. (2012). The role of SH3BP2 in the pathophysiology of cherubism. *Orphanet J. Rare Dis.* **7** Suppl. 1, S5.
Ren, J., Bharti, A., Raina, D., Chen, W., Ahmad, R. and Kufe, D. (2006). MUC1 oncoprotein is targeted to mitochondria by heregulin-induced activation of c-Src and the molecular chaperone HSP90. *Oncogene* **25**, 20-31.
Rich, M. M. and Lichtman, J. W. (1989). In vivo visualization of pre- and postsynaptic changes during synapse elimination in reinnervated mouse muscle. *J. Neurosci.* **9**, 1781-1805.
Sadoulet-Puccio, H. M., Rajala, M. and Kunkel, L. M. (1997). Dystrobrevin and dystrophin: an interaction through coiled-coil motifs. *Proc. Natl. Acad. Sci. USA* **94**, 12413-12418.
Salpeter, M. M., Cooper, D. L. and Levitt-Gilmour, T. (1986). Degradation rates of acetylcholine receptors can be modified in the postjunctional plasma membrane of the vertebrate neuromuscular junction. *J. Cell Biol.* **103**, 1399-1403.
Sanes, J. R. and Lichtman, J. W. (2001). Development: induction, assembly, maturation and maintenance of a postsynaptic apparatus. *Nat. Rev. Neurosci.* **2**, 791-805.
Schmidt, N., Akaaboune, M., Gajendran, N., Martinez-Pena y Valenzuela, I., Wakefield, S., Thurnheer, R. and Brenner, H. R. (2011). Neuregulin/ErbB regulate neuromuscular junction development by phosphorylation of alpha-dystrobrevin. *J. Cell Biol.* **195**, 1171-1184.
Schulze, W. X. and Mann, M. (2004). A novel proteomic screen for peptide-protein interactions. *J. Biol. Chem.* **279**, 10756-10764.
Shi, L., Fu, A. K. Y. and Ip, N. Y. (2012). Molecular mechanisms underlying maturation and maintenance of the vertebrate neuromuscular junction. *Trends Neurosci.* **35**, 441-453.
Siesser, P. F., Motolese, M., Walker, M. P., Goldfarb, D., Gewain, K., Yan, F., Kulikauskas, R. M., Chien, A. J., Wordeman, L. and Major, M. B. (2012). FAM123A binds to microtubules and inhibits the guanine nucleotide exchange factor ARHGEF2 to decrease actomyosin contractility. *Sci. Signal.* **5**, ra64.
Smith, C. L., Mittaud, P., Prescott, E. D., Fuhrer, C. and Burden, S. J. (2001). Src, Fyn, and Yes are not required for neuromuscular synapse formation but are necessary for stabilization of agrin-induced clusters of acetylcholine receptors. *J. Neurosci.* **21**, 3151-3160.
Song, W., Ren, D., Li, W., Jiang, L., Cho, K. W., Huang, P., Fan, C., Song, Y., Liu, Y. and Rui, L. (2010). SH2B regulation of growth, metabolism, and longevity in both insects and mammals. *Cell Metab.* **11**, 427-437.
Spangler, S. A. and Hoogenraad, C. C. (2007). Liprin-alpha proteins: scaffold molecules for synapse maturation. *Biochem. Soc. Trans.* **35**, 1278-1282.
Spangler, S. A., Jaarsma, D., De Graaff, E., Wulf, P. S., Akhmanova, A. and Hoogenraad, C. C. (2011). Differential expression of liprin-alpha family proteins in the brain suggests functional diversification. *J. Comp. Neurol.* **519**, 3040-3060.
Spangler, S. A., Schmitz, S. K., Kevenaar, J. T., de Graaff, E., de Wit, H., Demmers, J., Toonen, R. F. and Hoogenraad, C. C. (2013). Liprin-alpha2 promotes the presynaptic recruitment and turnover of RIM1/CASK to facilitate synaptic transmission. *J. Cell Biol.* **201**, 915-928.
Sunada, Y. and Campbell, K. P. (1995). Dystrophin-glycoprotein complex: molecular organization and critical roles in skeletal muscle. *Curr. Opin. Neurol.* **8**, 379-384.

Journal of Cell Science (2016) 129, 898-911 doi:10.1242/jcs.181180

Théard, D., Labarrade, F., Partisani, M., Milanini, J., Sakagami, H., Fon, E. A., Wood, S. A., Franco, M. and Luton, F. (2010). USP9x-mediated deubiquitination of EFA6 regulates de novo tight junction assembly. *EMBO J.* **29**, 1499-1509.

Vadlamudi, R. K., Sahin, A. A., Adam, L., Wang, R.-A. and Kumar, R. (2003). Heregulin and HER2 signaling selectively activates c-Src phosphorylation at tyrosine 215. *FEBS Lett.* **543**, 76-80.

Wiesner, C., Winsauer, G., Resch, U., Hoeth, M., Schmid, J. A., van Hengel, J., van Roy, F., Binder, B. R. and de Martin, R. (2008). Alpha-catulin, a Rho signalling component, can regulate NF-kappaB through binding to IKK-beta, and confers resistance to apoptosis. *Oncogene* **27**, 2159-2169.

Yang, B., Jung, D., Motto, D., Meyer, J., Koretzky, G. and Campbell, K. P. (1995). SH3 domain-mediated interaction of dystroglycan and Grb2. *J. Biol. Chem.* **270**, 11711-11714.

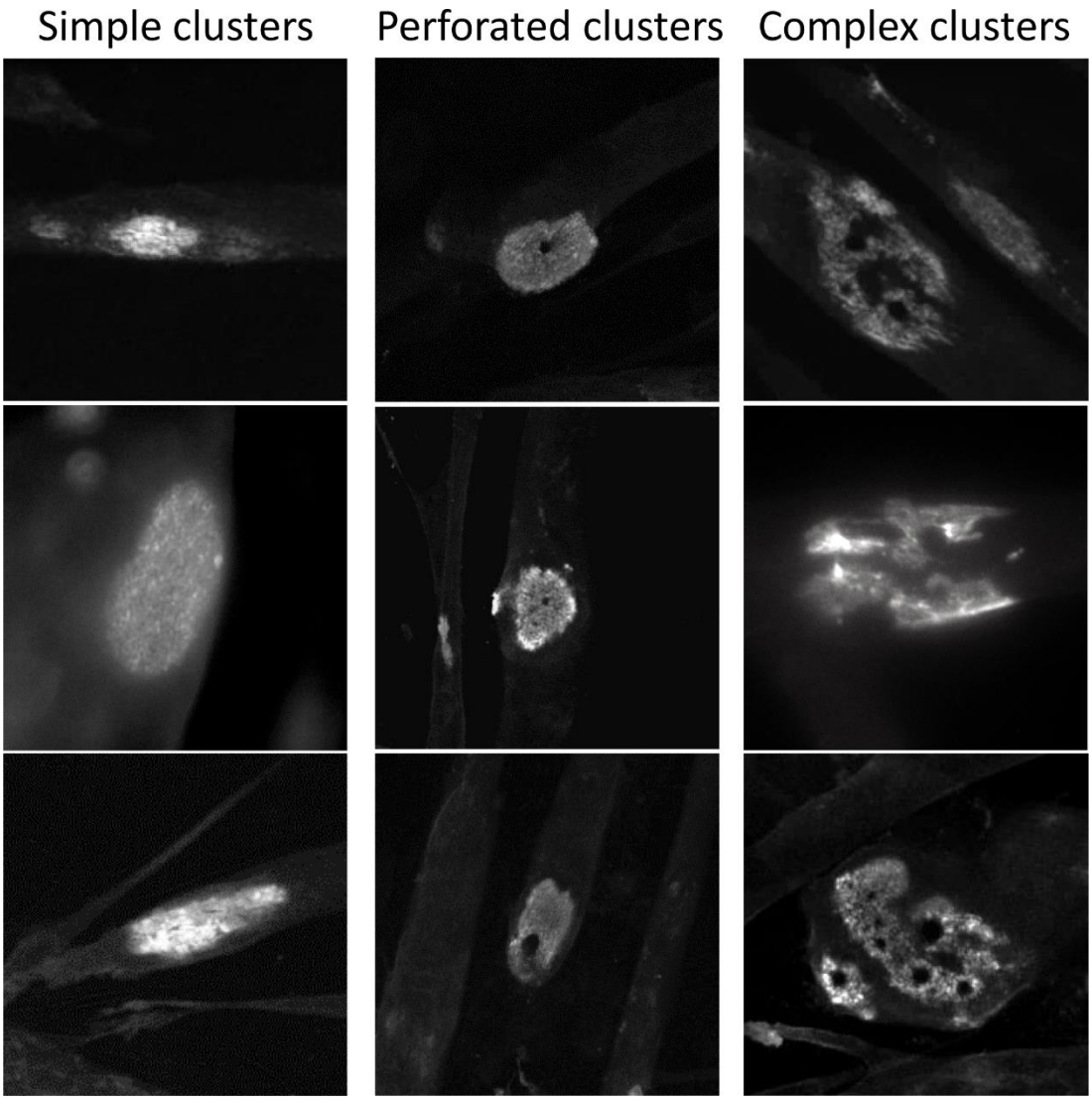

Figure S1. Examples of AChR clusters in primary myotubes that were classified as simple, perforated and complex.

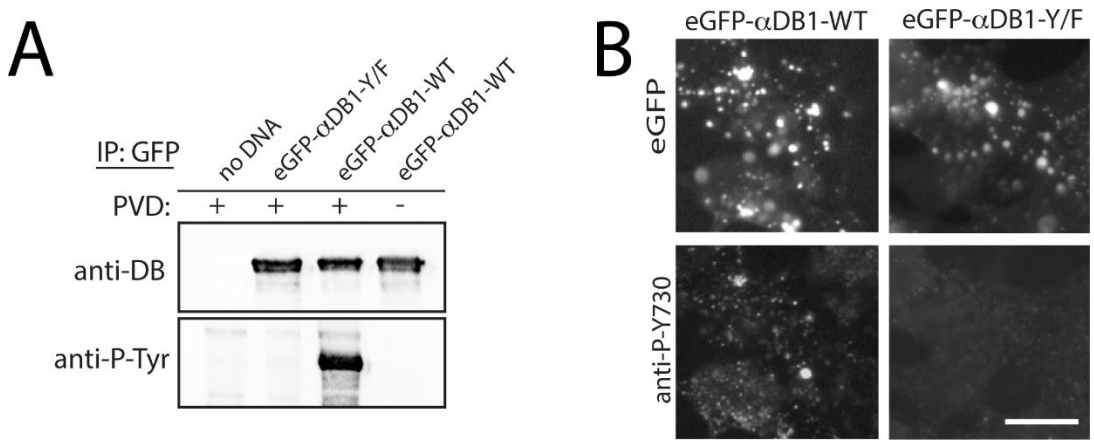

Figure S2. Evaluation of phospho-specific αDB-1 antibodies. (A) Pre-treatment of HEK293 cells with PVD increases level of αDB-1 phosphorylation. Lysates from PVD treated HEK293 cells transfected with indicated αDB-1 constructs was used to precipitate αDB-1 and the level of phosphorylation was analyzed with anti-phospho-tyrosine antibodies in Western blotting. (B) Anti-P-Y_{730} immunofluorescence was detected in HEK293 pervanadate (PVD) treated cells expressing eGFP-αDB1-WT, but not eGFP-αDB1-Y/F. Confirmation of expression of the corresponding proteins is shown by the eGFP signal.

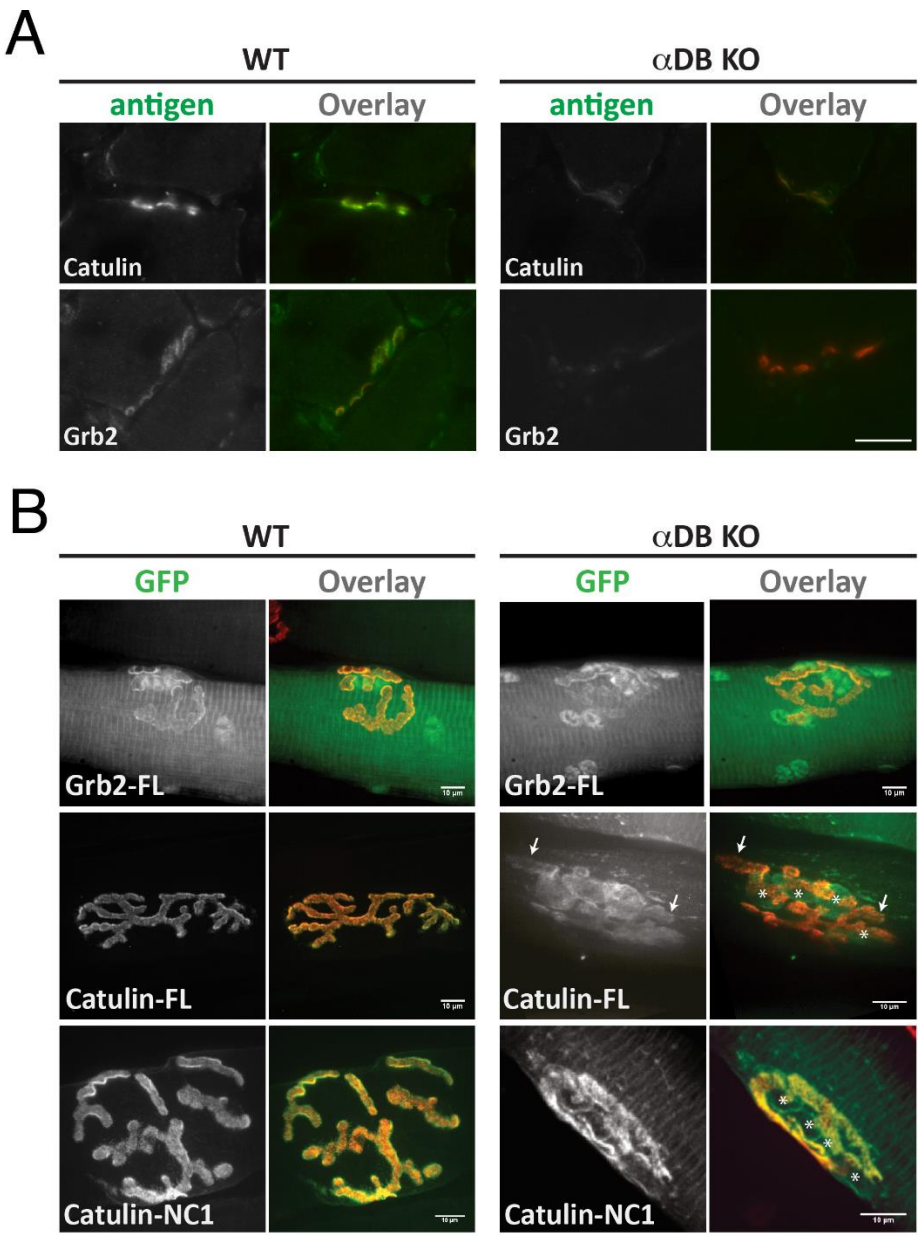

Figure S3. NMJ localization of α-catulin and Grb2 in αDB KO tissues. (A) immunolocalization of endogenous proteins (green) in 6 μm-thick cryostat cross-sections from *tibialis anterior* muscle from WT and αDB KO mice. (B) NMJ localization of indicated GFP-fusion constructs 10 days after electroporation into *tibialis anterior* muscles. Stars indicate position of synaptic nuclei that accumulate α-catulin in αDB KO tissues (not observed in tissues from WT animals); arrows indicate regions of the synapse with GFP fluorescence that is not obscured by overlapping localization of synaptic nuclei. BTX is shown in red; scale bar = 10 μm.